



1 Interactions between channels and
2 tributary alluvial fans: channel
3 adjustments and sediment-signal
4 propagation

5 Sara Savi¹, Stefanie Tofelde^{2,3}, Andrew D. Wickert⁴, Aaron Bufe³, Taylor F. Schildgen^{1,3}, and
6 Manfred R. Strecker¹

7 ¹Institut für Geowissenschaften, Universität Potsdam, 14476 Potsdam, Germany

8 ²Institut für Umweltwissenschaften und Geographie, Universität Potsdam, 14476 Potsdam,
9 Germany

10 ³Helmholtz Zentrum Potsdam, GeoForschungsZentrum (GFZ) Potsdam, 14473 Potsdam,
11 Germany

12 ⁴Department of Earth Sciences and Saint Anthony Falls Laboratory, University of Minnesota,
13 Minneapolis, MN 55455, USA

14 Corresponding Author: Sara Savi (savi@geo.uni-potsdam.de)

15

16 **Abstract**

17 Climate and tectonics impact water and sediment fluxes to fluvial systems. These boundary
18 conditions set river form and can be recorded by fluvial deposits. Reconstructions of boundary
19 conditions from these deposits, however, is complicated by complex channel-network
20 interactions and associated sediment storage and release through the fluvial system. To address
21 this challenge, we used a physical experiment to study the interplay between a main channel and
22 a tributary under different forcing conditions. In particular, we investigated the impact of a single
23 tributary junction, where sediment supply from the tributary can produce an alluvial fan, on
24 channel geometries and associated sediment-transfer dynamics. We found that the presence of an
25 alluvial fan may promote or prevent sediment to be moved within the fluvial system, creating
26 different coupling conditions. A prograding alluvial fan, for example, has the potential to disrupt



27 the sedimentary signal propagating downstream through the confluence zone. By analyzing
28 different environmental scenarios, our results indicate the contribution of the two sub-systems to
29 fluvial deposits, both upstream and downstream of the tributary junction, which may be
30 diagnostic of a perturbation affecting the tributary or the main channel only. We summarize all
31 findings in a new conceptual framework that illustrates the possible interactions between
32 tributary alluvial fans and a main channel under different environmental conditions. This
33 framework provides a better understanding of the composition and architecture of fluvial
34 sedimentary deposits found at confluence zones, which is essential for a correct reconstruction of
35 the climatic or tectonic history of a basin.

36

37 1. Introduction

38 The geometry of channels and the downstream transport of sediment and water in rivers are
39 determined by climatic and tectonic boundary conditions (Allen, 2008, and references therein).
40 Fluvial deposits and landforms such as conglomeratic fill terraces or alluvial fans may record
41 phases of aggradation and erosion that are linked to changes in sediment or water discharge, and
42 thus provide important archives of past environmental conditions (Armitage et al., 2011;
43 Castelltort and Van Den Driessche, 2003; Densmore et al., 2007; Mather et al., 2017; Rohais et
44 al., 2012; Tofelde et al., 2017). Tributaries are an important component of fluvial networks, but
45 their contribution to the sediment supply of a river channel can vary substantially (Bull, 1964;
46 Hooke, 1967; Lane 1955; Leopold and Maddock, 1953; Mackin, 1948; Miller, 1958). Their
47 impact on the receiving river (referred to as *main channel* hereafter) may not be captured by
48 numerical models of alluvial channels, as most models either parameterize the impacts of
49 tributaries into simple relationships between drainage-basin area and river discharge (Whipple
50 and Tucker, 2002; Wickert and Schildgen, 2019), or treat the main channel as a single channel
51 with no lateral input (e.g., Simpson and Castelltort, 2012). Extensive studies on river confluences
52 (e.g., Rice et al., 2008 and references therein) mainly focus on (1) hydraulic parameters of the
53 water flow dynamics at the junction (Best 1986, 1988), which are relevant for management of
54 infrastructure (e.g., bridges), and (2) morphological changes of the main channel bed, which are
55 relevant for sedimentological studies and riverine habitats (Benda et al., 2004a; Best 1986; Best



56 and Rhoads, 2008). Geomorphological changes (i.e., channel slope, width, or grain-size
57 distribution) have been studied in steady-state conditions only (Ferguson et al., 2006; Ferguson
58 and Hoey, 2008), and with no focus on fluvial deposits related to the interactions between
59 tributaries and the main channel. In source-to-sink studies an understanding of these processes,
60 however, is relevant for the reconstruction of the climatic or tectonic history of a certain basin.

61 By modulating the sediment supplied to the main channel, tributaries may influence the
62 distribution of sediment within the fluvial system and the origin and amount of sediment stored
63 within fluvial deposits at confluence zones. Additionally, complex feedbacks between tributaries
64 and main channels (e.g., Schumm, 1973; Schumm and Parker, 1973) may enhance or reduce the
65 effects of external forcing on the fluvial system, thus complicating attempts to reconstruct past
66 environmental changes from these sedimentary deposits.

67 The dynamics of alluvial fans can introduce an additional level of complication to the
68 relationship between tributaries and main channels. Fans retain sediment from the tributary and
69 influence the response of the connected fluvial system to environmental perturbations (Ferguson
70 and Hoey, 2008; Mather et al., 2017). Despite the widespread use of alluvial fans to decipher
71 past environmental conditions (Bull, 1964; Colombo et al., 2000; D’Arcy et al., 2017; Densmore
72 et al., 2007; Gao et al., 2018; Harvey, 1996; Savi et al., 2014; Schildgen et al., 2016), we still
73 lack a clear understanding of the interactions between alluvial fans and main channels under the
74 influence of different environmental forcing mechanisms. The lack of a systematic analysis of
75 these interactions represents a major gap in knowledge that hinders our understanding of (1) how
76 channels respond to changes in water and sediment supply at confluence zones, and (2) how
77 sediment moves within fluvial systems (Mather et al., 2017), with potential consequences for
78 sediment-transport dynamics as well as the composition and architecture of fluvial sedimentary
79 deposits.

80 In this study, we analyze the interplay between a main channel and a tributary under different
81 environmental forcing conditions in an experimental setting, with particular attention to
82 tributaries that generate an alluvial fan. Physical experiments have the advantage of providing a
83 simplified setting with controlled boundary conditions and that may include water and sediment
84 discharge, and uplift rate or base-level changes. These models may thus capture many

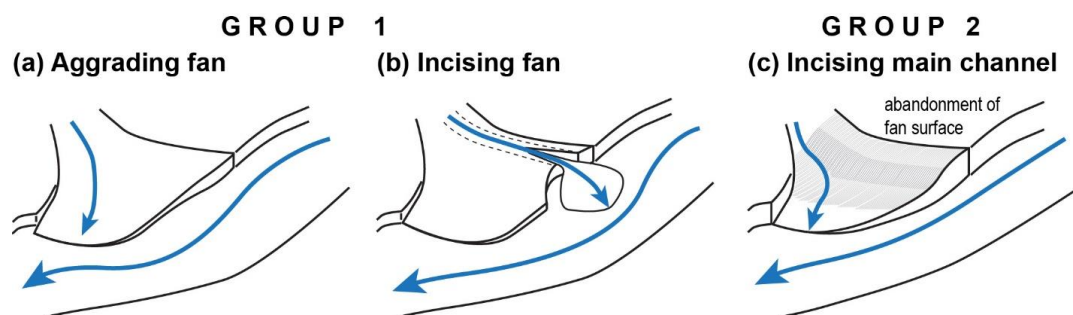


85 components of complex natural behaviors (Hooke, 1967; Paola et al., 2009; Schumm and Parker,
86 1973), and they provide an opportunity to analyze processes at higher spatial and temporal
87 resolution than is generally possible in nature (e.g., De Haas et al., 2016; Parker, 2010; Reitz et
88 al., 2010). These characteristics allow us to directly observe connections between external
89 perturbations (e.g., tectonic or climatic variations) and surface processes impacting landscapes.

90 We present results from two groups of experiments in which we separately imposed a
91 perturbation either in the tributary only (Group 1, Fig. 1a, b) or solely in the main channel
92 (Group 2, Fig. 1c). Group 1 can be further subdivided into cases in which the tributary has: (a) an
93 aggrading alluvial fan (Fig. 1a); or (b) an incising alluvial fan (Fig. 1b), whereas Group 2
94 represents a case of a sudden increase in water discharge in the main channel (Fig. 1c). These
95 three cases represent what may occur in many natural environments (e.g., Hamilton et al., 2013;
96 Leeder and Mack, 2001; Mather et al., 2017; Schumm 1973; Van Dijk et al., 2009).

97 By analyzing how a tributary may affect the main channel under these different forcing
98 conditions, we aim to build a conceptual framework that lends insight into the interplay between
99 alluvial fans and main channels. Toward this goal, we provide a schematic representation of how
100 the downstream delivery of sediment changes under different environmental conditions. Through
101 this representation, we hope to contribute to a better understanding and interpretation of fluvial
102 morphologies and sedimentary records, which may hold important information about regional
103 climatic and tectonic history (Allen, 2008; Armitage et al., 2011; Castelltort and Van Den
104 Driessche, 2003; Densmore et al., 2007; Mather et al., 2017; Rohais et al., 2012).

105



106



107 Figure 1. Schematic representation of the three scenarios analyzed in this study.

108

109 2. Background and Motivation

110 2.1. Geometry and sediment transfer dynamics in a single-channel system

111 2.1.1. General concepts

112 An alluvial river is considered to be in steady state (*equilibrium regime*) when its water
113 discharge provides sufficient power, or sediment-transport capacity, to transport the sediment
114 load supplied from the upstream contributing area at a given channel slope (Bull, 1979; Gilbert,
115 1877; Lane, 1955; Mackin, 1948). When that power is insufficient, sediment is deposited within
116 the channel (*aggradation*), whereas when the sediment-transport capacity exceeds the sediment
117 supply, the river erodes the channel banks and bed (*incision*) (Lane, 1955). Any change in
118 sediment or water supply modifies the sediment-to-water ratio, such that the river must
119 transiently adjust one or more of its geometric features (e.g., slope, width, depth, or grain-size
120 distribution) to re-establish equilibrium (Mackin 1948; Meyer-Peter and Müller, 1948).

121 When a perturbation occurs in the system, slope adjustments are not uniform along the
122 channel. If the perturbation occurs upstream (e.g., in water or sediment supply), channel slope
123 changes first at the channel head through incision or aggradation (e.g., Simpson and Castelltort
124 2012; Tofelde et al., 2019; Van den Berg Van Saparoea and Potsma, 2008; Wickert and
125 Schildgen, 2019). With time, slope adjustments proceed downstream until the entire channel
126 slope has adjusted to the new condition. Conversely, when perturbations occur downstream (e.g.,
127 a change in base level), the slope initially changes at the channel mouth, and the slope
128 adjustment propagates upstream until the entire channel is adjusted to the new base level (Parker
129 et al., 1998; Tofelde et al., 2019; Van den Berg Van Saparoea and Potsma, 2008; Whipple et al.,
130 1998).

131 At the scale of a drainage network, these geometric adjustments may alter the mechanisms
132 and rates at which sediment is moved across landscapes. In general, under both steady and
133 transient conditions, sediment moves from zones of erosion to areas of deposition passing



134 through a *transfer zone* (Castelltort and Van Den Driessche, 2003). The capacity of the transfer
135 zone to temporarily store or release sediment can influence the amount and the provenance of
136 sediment reaching the depositional zone, buffering the sedimentary signal carried through the
137 system (Tofelde et al., 2019). This buffering may be particularly important for the outcome of
138 analyses that use the geochemical composition of sediment (e.g., cosmogenic nuclide
139 concentrations) to date fluvial deposits or infer changes in erosion rate (Biermann and Steig,
140 1996; Granger et al., 1996, Lupker et al., 2012; Wittmann and von Blanckenburg, 2009;
141 Wittmann et al., 2011).

142 Although our understanding of buffering within the sediment-transfer zone helps to explain
143 how landscape perturbations are recorded in river morphology and downstream sedimentary
144 records, to date neither physical (Tofelde et al., 2019), theoretical (Castelltort and Van Den
145 Driessche, 2003; Paola et al., 1992; Wickert and Schildgen, 2019), nor numerical (Simpson and
146 Castelltort, 2012; Wickert and Schildgen, 2019) models take into account how the dynamics of
147 tributary junctions affect the geometry or sediment transport of the main channel. Tributary sub-
148 systems exist across spatial scales from small headwater catchments to continental-scale rivers
149 (i.e., short to large transfer zones). They may alter the amount of sediment entering the transfer
150 zone, modifying the sediment-input signals that can be recorded by fluvial terraces and
151 sedimentary basins. Understanding how tributaries and their fans interact with the main channel
152 is critical to correctly reconstruct external forcing conditions from the sediments of alluvial fans,
153 fluvial terraces, and depositional sinks.

154 2.1.2. *Alluvial fans*

155 Alluvial fans typically form at points of rapid decrease of channel slope and/or increases in
156 valley width (Benda, 2008; Bull, 1964). Their depositional processes are characterized by a
157 combination of sheet flows and channelized flows that are interrupted by large reorganizations of
158 the channel system through avulsions (Bryant et al., 1995; De Haas et al., 2016; Hooke and
159 Rohrer, 1979; Reitz et al., 2010; Reitz and Jerolmack, 2012). Variations in these processes can
160 be related to the internal, i.e. autogenic, dynamics of the system (Hamilton et al., 2013; Kim and
161 Jerolmack, 2008; Van Dijk et al., 2009, 2012) or to external forcings (Armitage et al., 2011;
162 Rohais et al., 2012). In general, sheet flows deposit sediment uniformly over the entire fan



163 surface. Conversely, channelization on fans is generally associated with localized erosion.
164 Avulsions are sudden reorganizations of the channel system that are integral to the cyclic
165 construction of a fan (Straub et al., 2009). They occur when channels aggrade above the fan
166 surface and suddenly change position to start deposition on a new location of the fan surface
167 (Hamilton et al., 2013; Van Dijk et al., 2009).

168 In our experiments, we distinguish between two modes of fan construction: *fan aggradation*,
169 i.e., deposition of material on the fan surface, which leads to an increase in the fan surface
170 elevation, and *fan progradation*, i.e., deposition that occurs at the downstream margin of the fan,
171 which leads to fan lengthening. Progradation may occur during both aggradation and incision
172 phases (Fig. 1).

173 2.2. Geometry and sediment-transfer dynamics in a multi-channel system

174 2.2.1. Tributary influence on main channel

175 At confluence zones, the main channel is expected to adapt its width, slope, transport rate,
176 and sediment-size distribution according to the combined water and sediment supply from the
177 main channel and the tributary (Benda et al., 2004b; Best, 1986; Ferguson et al., 2006; Lane
178 1955; Miller, 1958; Rice et al., 2008). Consequently, a perturbation occurring in the tributary
179 will also affect the main channel. For example, a sudden increase in sediment input from a
180 tributary (e.g., from a landslide or debris flow) can overwhelm the transport capacity of the main
181 channel, thereby inducing sediment deposition at the confluence (Fig. 1a). As a result, the main
182 channel upstream of the tributary experiences a rise in its local base level, which causes
183 additional local deposition and a transient reduction in the main-channel slope upstream of the
184 tributary (Ferguson et al., 2006; Benda, 2008; Benda et al., 2004b). This sediment deposition
185 upstream from the tributary increases the slope of the main channel downstream of the tributary,
186 until the main channel is adjusted to transporting the higher sediment load (Benda et al., 2003;
187 Ferguson et al., 2006; Ferguson and Hoey, 2008; Mackin, 1948; Rice and Church, 2001). It
188 follows that the main channel both upstream and downstream from the tributary should undergo
189 an aggradation phase, the former due to an increase in its local base level at the junction, the
190 latter because of an increase in sediment supply from the tributary (Ferguson and Hoey, 2008;
191 Mackin, 1948; Rice and Church, 2001). In their numerical model, Ferguson et al. (2006) found



192 that when tributaries cause aggradation at the junction with the main channel, the main channel
193 slope adjustments extend approximately twice as far upstream as they do downstream. They
194 additionally found that variations in grain-size input from a tributary influence the grain-size
195 distribution in the main channel, both upstream and downstream of the tributary junction.
196 Considering that in our experiments we used a homogeneous grain size, the work of Ferguson et
197 al. (2006) complements our analyses.

198 Whether the tributary is aggrading, incising, or in equilibrium may also have important
199 consequences for *how* and *where* local fluvial deposits (i.e., alluvial-fan deposits or fluvial
200 terraces) reflect environmental signals. For example, when sediment is trapped within a
201 tributary's alluvial fan, the fan acts as *buffer* for the main channel, and environmental signals do
202 not propagate from the tributary into the fluvial deposits of the main channel (Ferguson and
203 Hoey, 2008; Mather et al., 2017). In contrast, where the tributary and main channel are fully
204 *coupled* (i.e. all sediment mobilized in the tributary reaches the main channel), the signal
205 transmitted from the tributary can be recorded in the stratigraphy of the main river (Mather et al.,
206 2017). Hence, to correctly interpret fluvial deposits and to reduce ambiguity, an understanding of
207 the aggradational/incisional state of the tributary and how this state influences the main channel
208 is important. In this study, we aim to provide this information for different tributary states.

209 2.2.2. *Main channel influence on tributary*

210 The main channel influences a tributary primarily by setting its local base level. Therefore, a
211 change in the main-channel bed elevation through aggradation or incision represents a
212 downstream perturbation for the tributary, and tributary-channel adjustments will follow a
213 *bottom-up* propagation direction (Mather et al., 2017; Schumm and Parker, 1973). Typically, a
214 lowering of the main channel produces an initial phase of tributary-channel incision (Cohen and
215 Brierly, 2000; Fulkner et al., 2016; Germanoski and Ritter, 1988; Heine and Lant, 2009; Ritter et
216 al., 1995; Simon and Rinaldi, 2000), followed by channel widening (Cohen and Brierly, 2000;
217 Germanoski and Ritter, 1988), which occurs mainly through bank erosion and mass-wasting
218 processes (Simon and Rinaldi, 2000). As base-level lowering continues, the fan may become
219 entrenched, with the consequent abandonment of the fan surface and renewed deposition at a
220 lower elevation (Clark et al., 2010; Mather et al., 2017; Mouchen  et al., 2017; Nicholas et al.,



221 2009) (Fig. 1c). In contrast, aggradation of the main channel may lead to tributary-channel
222 backfilling and avulsion (Bryant et al., 1995; De Haas et al., 2016; Hamilton et al. 2013; Kim
223 and Jerolmack, 2008; Van Dijk et al., 2009, 2012).

224 When a non-incising main channel (*non-incising main axial river* of Leeder and Mack, 2001)
225 is characterized by efficient lateral erosion, it can efficiently erode the fan downstream margin,
226 thereby “cutting” its toe (Larson et al., 2015) (*fan-toe cutting* hereafter) (Fig. 1b). This toe-
227 cutting shortens the fan and increases the tributary channel slope. As a consequence, the increase
228 in transport capacity in the tributary triggers an upstream-migrating wave of incision. Fan-toe
229 cutting may thus cause fan incision and a consequent increase in sediment supply from the
230 tributary to the main channel (*healing wedge* hereafter; Leeder and Mack, 2001), in a process
231 similar to that caused by an incising main channel (*incising main axial river* of Leeder and Mack,
232 2001).

233 2.2.3. Main channel and tributary interactions

234 Changes that occur in the tributary as a consequence of incision of the main channel may
235 alter the sediment supplied to the main river and create a series of autogenic feedback processes
236 that are generally referred to as a *complex response* (Schumm, 1973; Schumm and Parker, 1973).
237 These processes may form landforms such as cut-and-fill terraces that are not directly linked to
238 the original perturbation (Schumm, 1973), thereby complicating the reconstruction of past
239 environmental changes from such landforms. In our experiments, we analyze the changes
240 occurring in a tributary during a phase of main-channel incision to evaluate these potential
241 feedbacks.

242 3. Methods

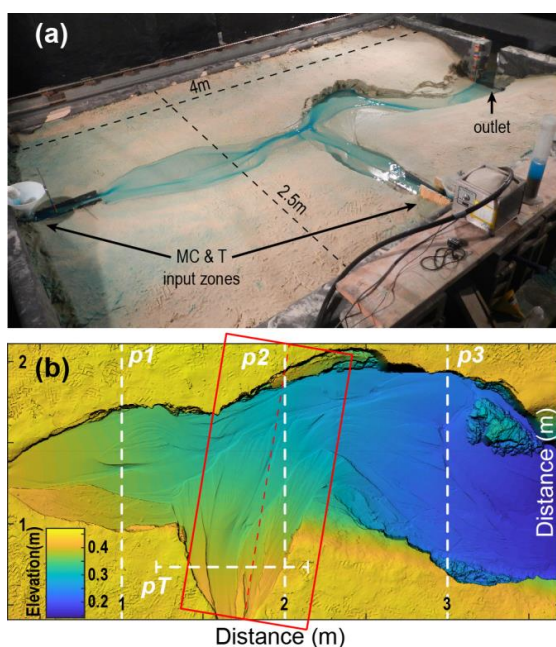
243 3.1. Experimental setup

244 We conducted physical experiments at the Saint Anthony Falls Laboratory (Minneapolis,
245 USA). The experimental setup consisted of a wooden box with dimensions of 4 m x 2.5 m x 0.4
246 m, which was filled with quartz sand with a mean grain size of 144 μm (standard deviation of 40
247 μm). Two separate water and sediment input zones were used to form a main channel (MC) and



248 a tributary channel (T) (Fig. 2a). The main channel's input zone was located along the short side
249 of the box, whereas the tributary's input zone was located along the long side at a distance of 1.7
250 m downstream of the main-channel inlet (Fig. 2a). For each of the two input zones, the water
251 supply (Q_w) and sediment supply (Q_{s_in}) could be regulated separately, and sand and water were
252 mixed before entering the box by feeding them through cylindrical wire-mesh diffusers filled
253 with gravel. Before entering the mesh, water was dyed blue to be visible on photos. At the
254 downstream end, sand (Q_{s_out}) and water exited the basin through a 20 cm-wide gap that opened
255 onto the floor below. This downstream sink was required to avoid deltaic sediment deposition
256 that would, if allowed to grow, eventually raise the base level of the fluvial system. At the
257 beginning of each experiment, an initial channel was shaped by hand to allow the water to flow
258 towards the outlet of the box.

259



260

261 Figure 2. Experimental set-up. (a) Wooden box for the experiments showing the two zones of
262 sediment and water input, and the outlet of the basin. (b) Digital elevation model constructed
263 from laser scans (1 mm horizontal resolution). Red box shows the area of the swath grid used for
264 the calculation of the tributary long profile (Fig. 4) and slope values. Dashed white lines
265 represent the location of the cross sections shown in Figs. 5 and 6.



266

267 3.2. Boundary conditions

268 We performed six experiments with different settings and boundary conditions to simulate
269 different tributary–main-channel interactions. As a reference, we included one experiment
270 without a tributary and with a constant Q_{s_in} and Q_w (MC_NC, where MC stands for *Main*
271 *Channel only* and the suffix NC stands for *No Change* in boundary conditions; reported in
272 Tofelde et al., 2019 as the Ctrl_2 experiment). The other five experiments all have a tributary
273 and are divided into two groups: In Group 1, Q_w and Q_{s_in} on the main channel were held
274 constant, whereas we varied these inputs to the tributary. In Group 2, Q_w and Q_{s_in} on the
275 tributary were held constant, whereas we increased Q_w in the main channel. In natural systems,
276 changes in water and sediment supply may affect the main channel and tributary simultaneously,
277 but to isolate the effects of the main channel and the tributary on each other, we studied
278 perturbations that only affect one of them at a time. Our results can be combined to predict the
279 response to a system-wide change in boundary conditions.

280 Each group includes one experiment with no change (NC) in Q_{s_in} and Q_w (T_NC1 and
281 T_NC2, where T stands for *run with Tributary* and the numbers at the end correspond to the
282 group number). Group 1 includes one experiment with an increase followed by a decrease in
283 Q_{s_in} in the tributary (T_ISDS, where ISDS stands for *Increasing Sediment Decreasing Sediment*)
284 and one experiment with a decrease followed by an increase in Q_w in the tributary (T_DWIW,
285 where DWIW stands for *Decreasing Water Increasing Water*). Changes were first made in the
286 direction that favored sediment deposition and the construction of an alluvial fan. Group 2
287 includes one experiment with no change (T_NC2) and one with an increase in Q_w in the main
288 channel (T_IWMC, where IWMC stands for *Increasing Water in Main Channel*). Importantly,
289 the initial settings of the two groups of experiments are different (Table 1). In particular, initial
290 Q_w and Q_{s_in} of Group 2 guarantee a higher Q_s/Q_w ratio, so that we could evaluate the effects of a
291 change in the main-channel regime (from a *non-incising main river* to an *incising main river*) on
292 the tributary and on sediment-signal propagation. In the context of this coupled tributary–main-
293 channel system, we explore: 1) the geometric variations that occur in the main channel and in the



294 tributary (e.g., channel slope and valley geometry); and 2) the downstream delivery of sediment
 295 and sedimentary signals.

296 **Table 1.** Overview of input parameters.

| EXP NAME | Initial conditions | | | | 1 st change | | | 2 nd change | |
|--|--------------------|-------|------|-------|------------------------|------|-------|-----------------------------|-------|
| | MC | | T | | MC Qw | T | | T | |
| | Qw | Qs_in | Qw | Qs_in | | Qw | Qs_in | Qw | Qs_in |
| | mL/s | mL/s | mL/s | mL/s | mL/s | mL/s | mL/s | mL/s | mL/s |
| MC_NC** | 95 | 1.3 | | | | | | | |
| <i>Non-incising mean axial rivers – Group1</i> | | | | | <i>(at 300 min)</i> | | | <i>(at 375* or 480 min)</i> | |
| T_NC1 | 95 | 1.3 | 63 | 2.2 | | | | | |
| T_ISDS | 95 | 1.3 | 63 | 2.2 | | | 4.5 | | 2.2 |
| T_DWIW* | 95 | 1.3 | 63 | 2.2 | | 31.5 | | 63 | |
| <i>Incising mean axial rivers - Group2</i> | | | | | <i>(at 180 min)</i> | | | | |
| T_NC2 | 63 | 1.3 | 41.5 | 2.2 | | | | | |
| T_IWMC | 63 | 1.3 | 41.5 | 2.2 | 126 | | | | |

297 * In the T_DWIW run the boundary condition change occurred at 375 min rather than 480 min
 298 as in the T_ISDS experiment because fast aggradation that occurred at the tributary input zone
 299 risked to overtop the wooden box margins.

300 **, Experiment published by Tofelde et al. (2019).

301

302 3.3. Measured and calculated parameters

303 3.2.1. Long profiles, valley cross-sections, and slope values

304 Every 30 min we stopped the experiments to perform a scan with a laser scanner mounted
 305 on the railing of the basin that surrounded the wooden box. Digital elevation models (DEMs)
 306 created from the scans have a resolution of 1 mm (Fig. 2b). We extracted long profiles and valley
 307 cross sections from these DEMs (i.e., elevation profiles perpendicular to the main flow direction)
 308 for the main channel and the tributary. Long profiles for the main channel were calculated by
 309 extracting the lowest elevation point along each cross section along the flow direction. Long
 310 profiles for the tributary were calculated with a similar procedure using outputs from



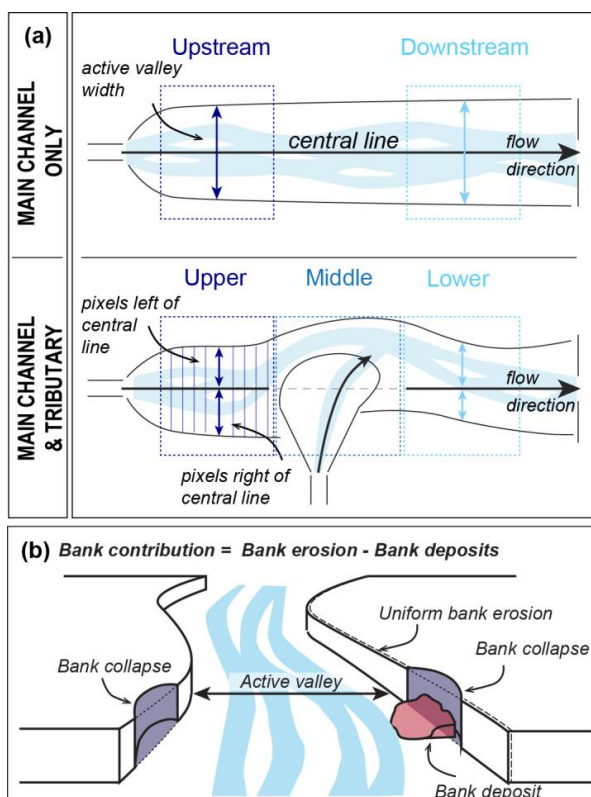
311 Topotoolbox's SWATH profile algorithm (Schwanghart and Scherler, 2014) at 1 mm spatial
312 resolution along the line of the average flow direction (Fig. 2b). By plotting elevation against
313 down-valley or down-fan distance, rather than along the evolving path of the channels, the
314 resulting slopes are slightly overestimated due to the low sinuosity of the channels. Cross
315 sections were extracted at fixed positions, perpendicular to the main flow direction, for both the
316 main channel and the tributary (Fig. 2b).

317 For the main channel, spatially-averaged slopes were additionally calculated by manually
318 measuring the bed elevation at the inlet and at the outlet of the wooden box at 10-minute
319 intervals during the experiments. This procedure yielded real-time estimates of channel slope.
320 For comparison, spatially-averaged slopes were subsequently calculated also for the tributary
321 channel using the maximum and minimum elevation of the tributary long profile calculated
322 within the SWATH grid. Slope data are reported in the supplementary material.

323 3.2.2. *Active valley-floor width and symmetry*

324 We defined the width of the active valley floor as the area along the main channel that was
325 occupied at least once by flowing water. It was measured along the main channel both upstream
326 and downstream of the tributary junction (Fig. 3a, upper panel). The active valley floor was
327 isolated by extracting all DEM values with an elevation of <0.42 m (where 0.42 m is the
328 elevation of the sand surface outside the manually-shaped channel) and with a slope of <15
329 degrees (a value visually selected from the DEMs as the best cut-off value for distinguishing the
330 valley floor from the banks). The average valley-floor width values were then calculated as the
331 average sum of pixels in each of the 700 cross sections within the selected zones (i.e., upstream
332 or downstream of the tributary junction; Fig. 3a, upper panel). The same method was used to
333 monitor valley symmetry. In this case, the averaged width was limited to the sum of pixels to the
334 left and to the right of an imaginary central line crossing the basin from the inlet to the outlet
335 (Fig. 3a). Small differences between left and right sums indicate high symmetry.

336



337

338 Figure 3. (a) Schematic representation of the method used to calculate the active valley width
339 and symmetry. Symmetry and averaged width values are calculated for 700 cross sections
340 located within the boxes marked in the upper panel. The averaged position of the valley margins
341 with respect to an imaginary central line, which connects the source zone to the outlet of the
342 wooden box, is shown in Figure 7. This representation highlights the symmetry of the valley and
343 indirectly provides the valley width (i.e., sum of the right and left-margin positions). Boxes
344 marked in the lower panel show the division in Upper, Middle, and Lower sections used for the
345 calculation of the mobilized volumes (Fig. 9). (b) Schematic representation of the method used to
346 calculate bank contribution: Elevation difference > -2.5 cm represents bank erosion and bank
347 collapses, whereas differences > 2.5 cm represent large bank deposits. The contribution of the
348 banks is calculated by subtracting these two values.

349



350 3.2.3. *Sediment discharge at the outlet (Q_{s_out}), mobilized volumes, and bank*
351 *contribution*

352 The sediment discharge at the outlet of the basin (Q_{s_out}) was manually recorded at 10-minute
353 intervals by measuring the volume of sediment that was collected in a container over a 10-second
354 period. Q_{s_out} was also calculated by differencing subsequent DEMs (generating a “DEM of
355 Difference”, or DoD) and calculating the net change in sediment volume within the DEM.
356 Although having a lower temporal resolution than the manual measurements (i.e., DoDs are
357 averaged over 30 minutes), this DEM-based calculation allowed us to identify zones of
358 aggradation and incision within the system and calculate their volumes. For each DoD, we
359 distinguished between changes along the active valley floor due to channel dynamics (elevation
360 difference < 2.5 cm, value chosen as best cut-off value) and changes that occur along the channel
361 and valley walls, for example due to bank collapses (elevation difference > 2.5 cm). Changes
362 within the active valley floor were further divided into areas of net *aggradation* ($\Delta V_{vf} > 0$) and
363 *erosion* ($\Delta V_{vf} < 0$). Changes in bank elevation were divided into *bank deposition* ($\Delta V_b > 0$) and
364 *bank collapses* or *erosion* ($\Delta V_b < 0$). These were used to calculate the bank contribution (V_b) to
365 the total volume (V) of mobilized sediment (Fig. 3b). We separated the upper, middle, and lower
366 sections of the experimental river valley by dividing the DEMs into three different zones (Fig.
367 3a, lower panel). For each section, we calculated the volume of sediment moved between two
368 time steps within the active valley floor (V_{vf}), along the banks (V_b), and the sum of the two
369 contributions ($V = V_{vf} + V_b$).

370 The volumes are normalized to the Q_{s_in} measured over 30 minutes (to match the 30-minute
371 period of a DoD). Negative V values indicate net incision, whereas positive values indicate net
372 aggradation. V values close to zero may indicate that there was no change, or that the net incision
373 \cong net aggradation. As such, it is important to look at the variations through time rather than at
374 single values.



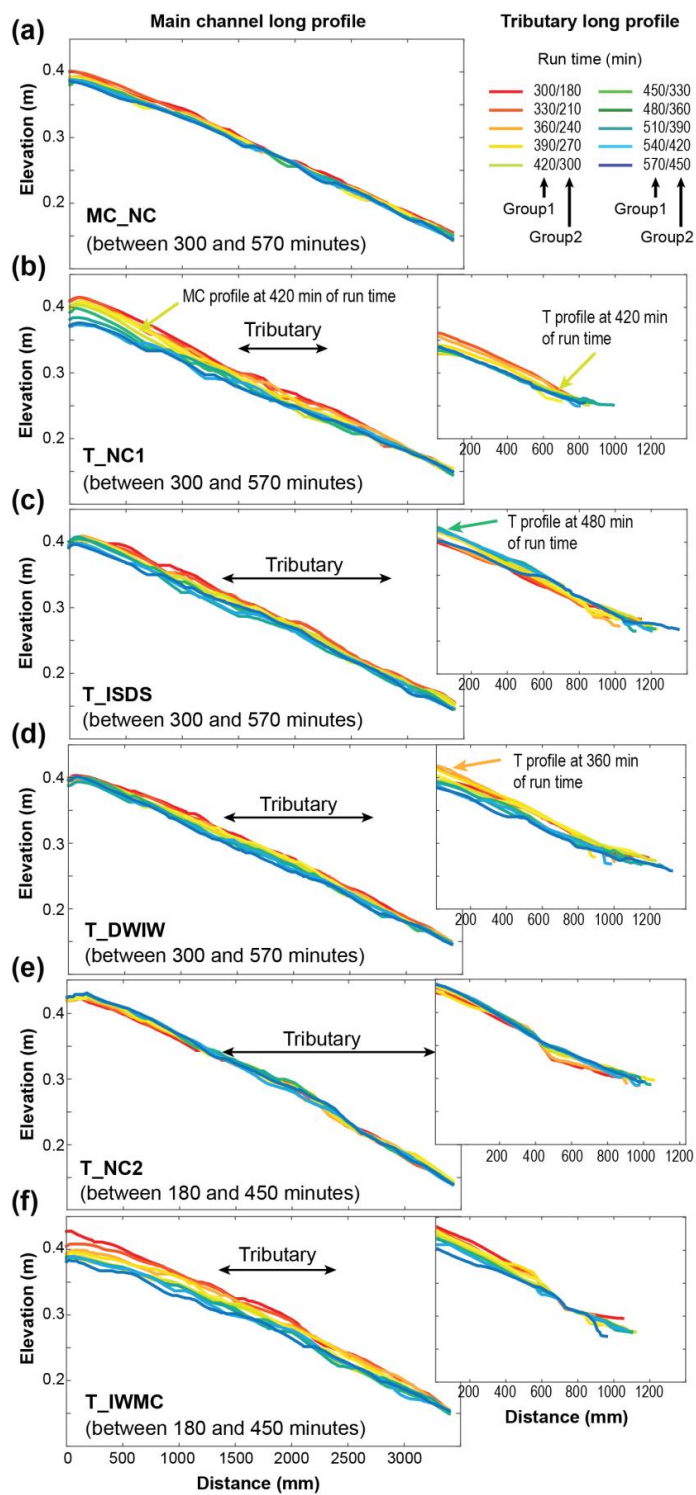
375 4. Results

376 All experiments included an initial adjustment phase characterized by high Q_{s_out} and a
377 short and rapid increase in the main-channel slope through preferential channel incision at the
378 downstream end of the main channel. This phase represents the adjustment from the manually
379 constructed valley shape to the shape that is equilibrated to the imposed boundary conditions. At
380 the start of the adjustment phase, the channel rapidly incised toward the outlet, which was much
381 lower than the height of the manually constructed valley bottom, meanwhile depositing material
382 at the channel head adjusting to the Q_{s_in} and Q_w values. Analogous to a base-level fall observed
383 in nature, this caused an increase in main-channel slope near the outlet and the upstream
384 migration of a diffuse knick-zone that lowered the elevation of the main channel. After this
385 initial adjustment, which marks the end of the spin-up phase, the main controlling factors for the
386 shape of the channel were the Q_{s_in} and Q_w values only.

387 4.1. Geometric adjustments

388 Channel-slope adjustments in our experiments followed the theoretical models described
389 above (Section 2.1). Following the spin-up phase, the main-channel slope decreased in all
390 experiments through incision at the upstream end, except for T_NC2 and the initial phase of
391 T_IWMC, in which the boundary conditions favored aggradation (Fig. 4, Table 1). The slope of
392 the tributary increased during periods of fan aggradation (e.g., IS phase of the T_ISDS run, and
393 DW phase of the T_DWIW run) and decreased during periods of fan incision (DS phase of the
394 T_ISDS run, and IW phase of the T_DWIW run) (Fig. 4). Slope adjustments did not occur
395 uniformly, but followed a top-down or bottom-up direction depending on the origin of the
396 perturbation (e.g., changes in headwater conditions or base-level fall at the tributary outlet).

397



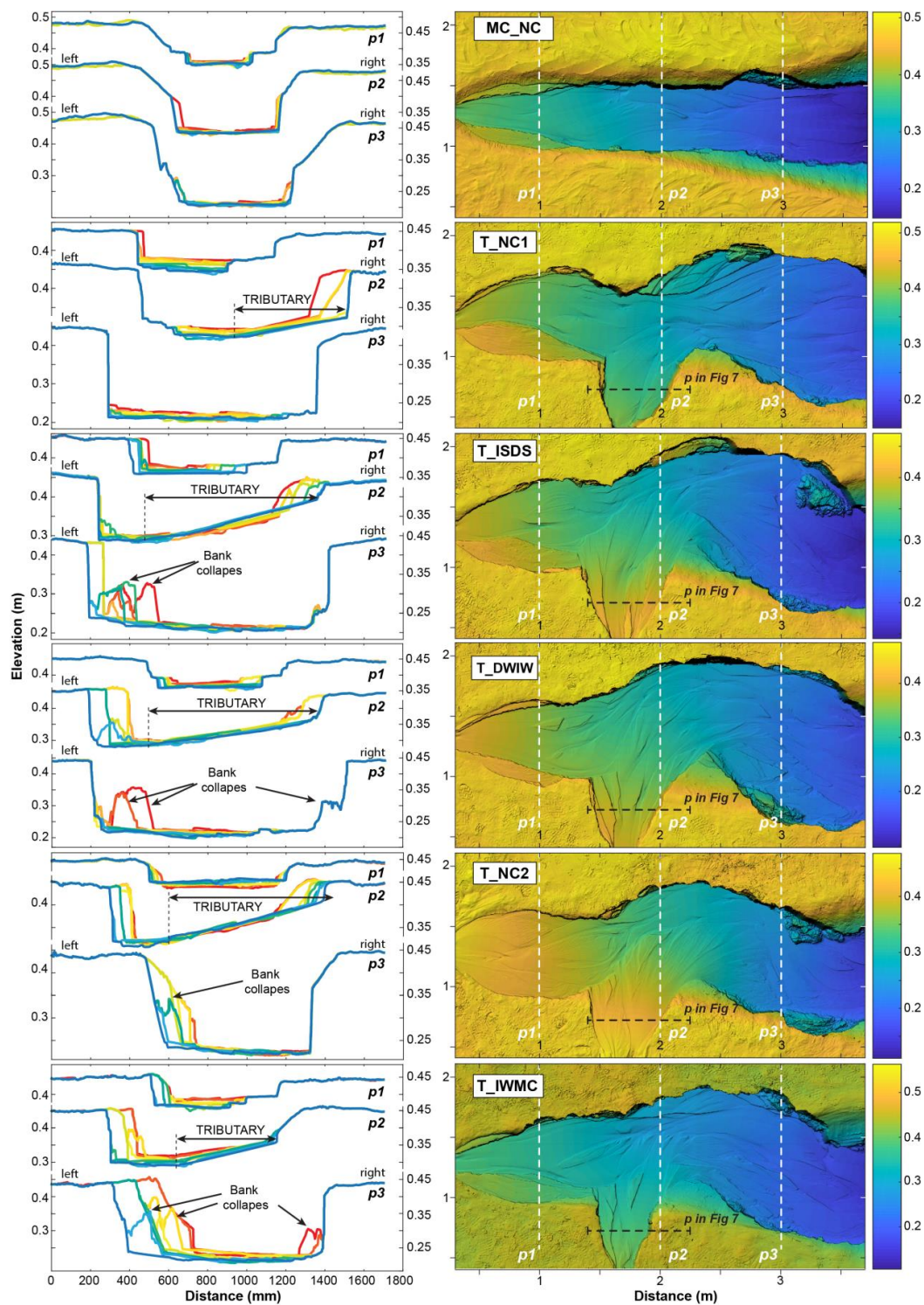


399 Figure 4. Long profiles of the main channel (left panels) and of the tributary channel (right
400 panels) for all runs. Profiles represent the experiments between 300 and 570 minutes for the
401 MC_Ctrl2, T_NC1, T_ISDS, and T_DWIW runs (legend values to the left of the slashes), and
402 between 180 and 450 minutes for the T_NC2, and T_IWMC runs (legend values to the right of
403 the slashes). Along the main channel profiles, horizontal arrows indicate the position and extent
404 of the tributary channel/alluvial fan, whereas colored arrows indicate the position of the channels
405 in particular run times discussed in the text.

406

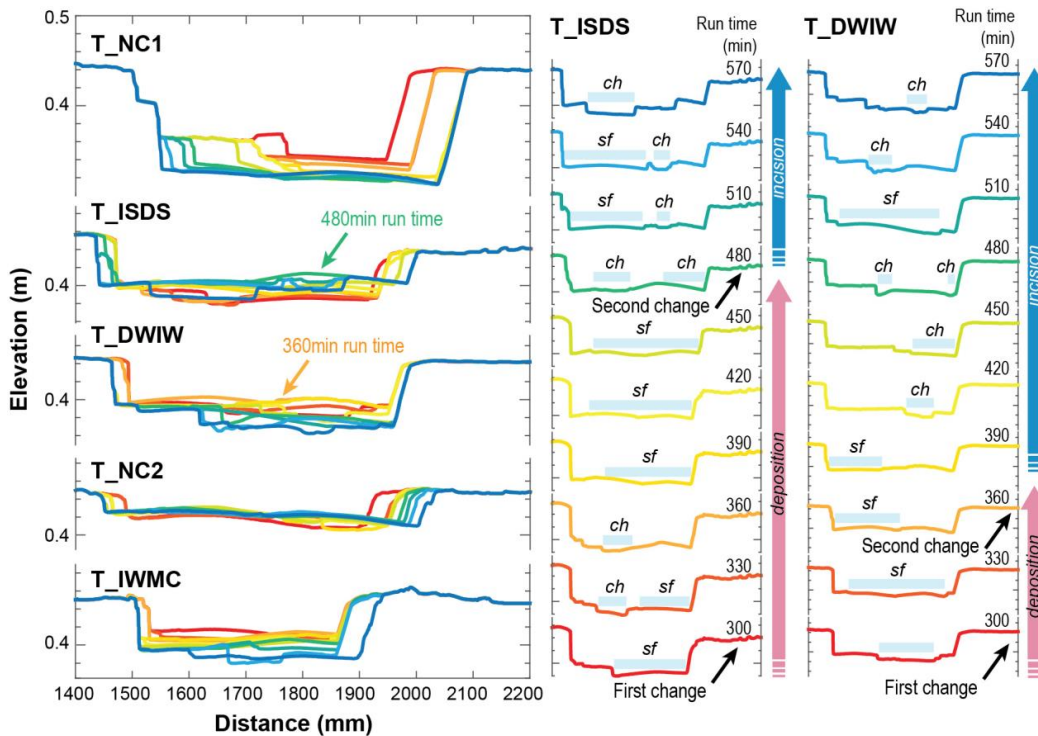
407 Valley width in both the main channel (Fig. 5) and the tributary (Fig. 6) increased during the
408 experiments, mainly through bank erosion and bank collapses, until reaching relatively steady
409 values (Fig. 7). The experiments with the tributary (Fig. 7b – f) developed a much wider main-
410 channel valley, especially downstream of the tributary, where Q_w was increased > 60% by the
411 additional Q_w input from the tributary. In these experiments, valleys were also strongly
412 asymmetrical, with more erosion affecting the valley side opposite the tributary (Figs. 5 and 7).

413





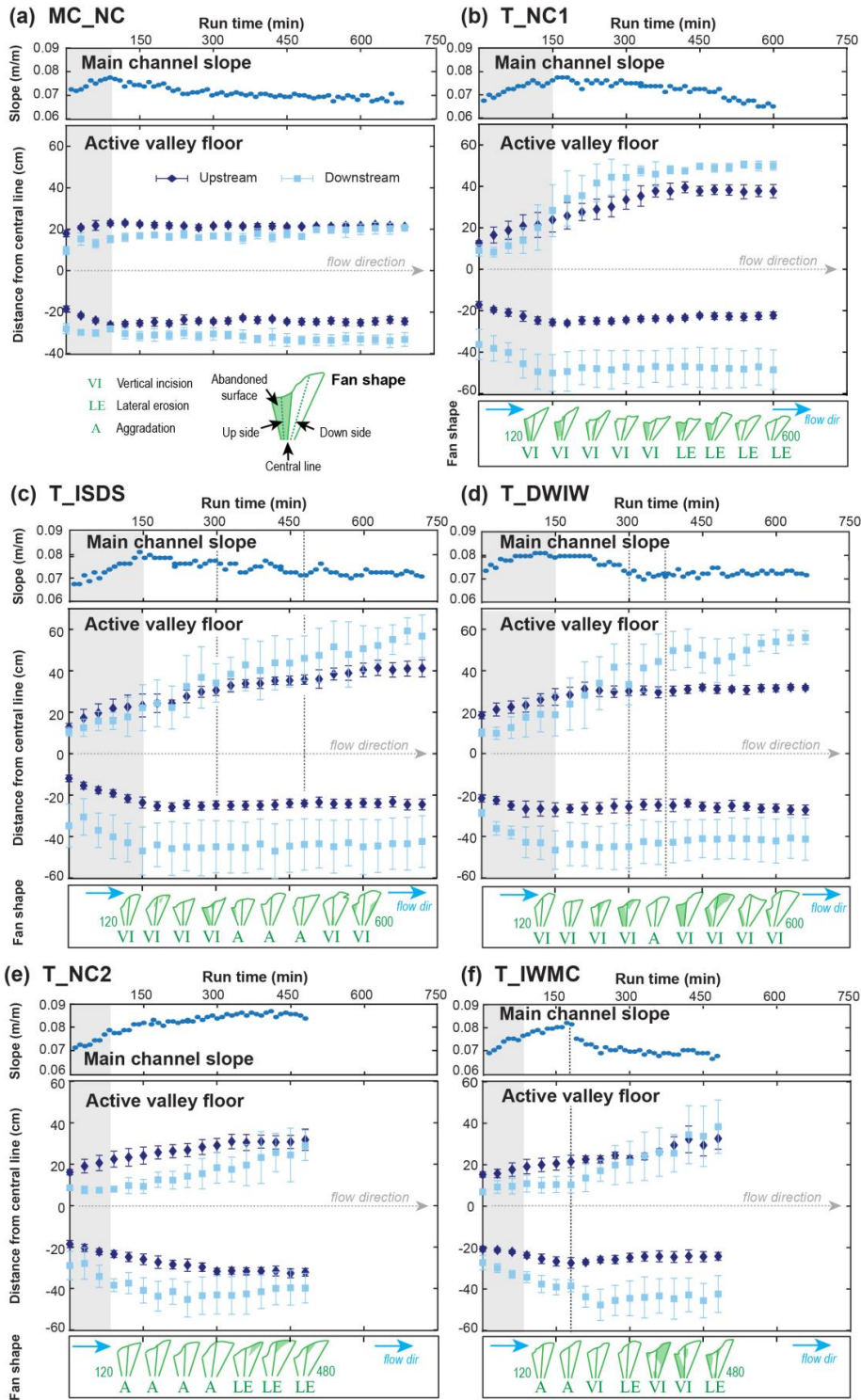
415 Figure 5. Left panels: Cross sections obtained from the DEMs at three different locations along
 416 the main channel (p1, p2, and p3 respectively). The color code represents successive DEMs as
 417 illustrated in Fig. 4 (i.e., same colors for the same run times). All cross sections are drawn from
 418 left to right looking in the downstream direction. Right panels: DEM maps expressed in meters;
 419 color code represents the elevation with respect to the channel floor (also in meters).



420

421 Figure 6. Cross sections in the tributary drawn from left to right looking downstream. The left
 422 panels show the evolution of all runs (color code as in Fig. 4 and 5); the right panels show the
 423 evolution of the T_ISDS and T_DWIW runs in more detail: the ground-surface elevation
 424 (colored lines) and the wetted areas (light blue bars) are shown. During aggradation, sheet flows
 425 (*sf*) dominate the transport mode of sediment, although channels (*ch*) may contemporaneously be
 426 present on the fan surface. During incision, the flow alternates between channelized flows and
 427 sheet flows and contribute to lowering the entire fan topography.

428





430 Figure 7. Variations in the geometry of the active valley floor for all experiments. For each
431 experiment the upper panel shows the measured slope (measured every 10 minutes during each
432 experimental run). The middle panel shows the calculated average position of the right and left
433 valley margins with respect to the central line, respectively for the main channel upstream and
434 downstream of the tributary junction (as indicated in Fig. 3a). Gray areas represent the spin-up
435 phase of each experiment (based on the break-in-slope registered through the manual slope
436 measurements; (a–f) upper panels). Vertical dotted lines in the T_ISDS, T_DWIW, and
437 T_IWMC runs represent the *time of change* in boundary conditions. Values are reported with
438 their relative 1σ value. For all experiments with a tributary, the shape of the fan and the dominant
439 sedimentary regime acting in the tributary at that specific time (i.e., vertical incision (VI), lateral
440 erosion (LE), or aggradation (A)) is shown in the lower panel. In all experiments, fan-toe cutting
441 (Leeder and Mack, 2001; Larson et al., 2015) mainly occurred at the upstream margin of the fan
442 and contributed to the strong asymmetry of the fan morphology (Table S9 of Supp. Material),
443 similar to what has been observed in nature (Giles et al., 2016).

444

445 4.2. $Q_{s,out}$ and bank contribution

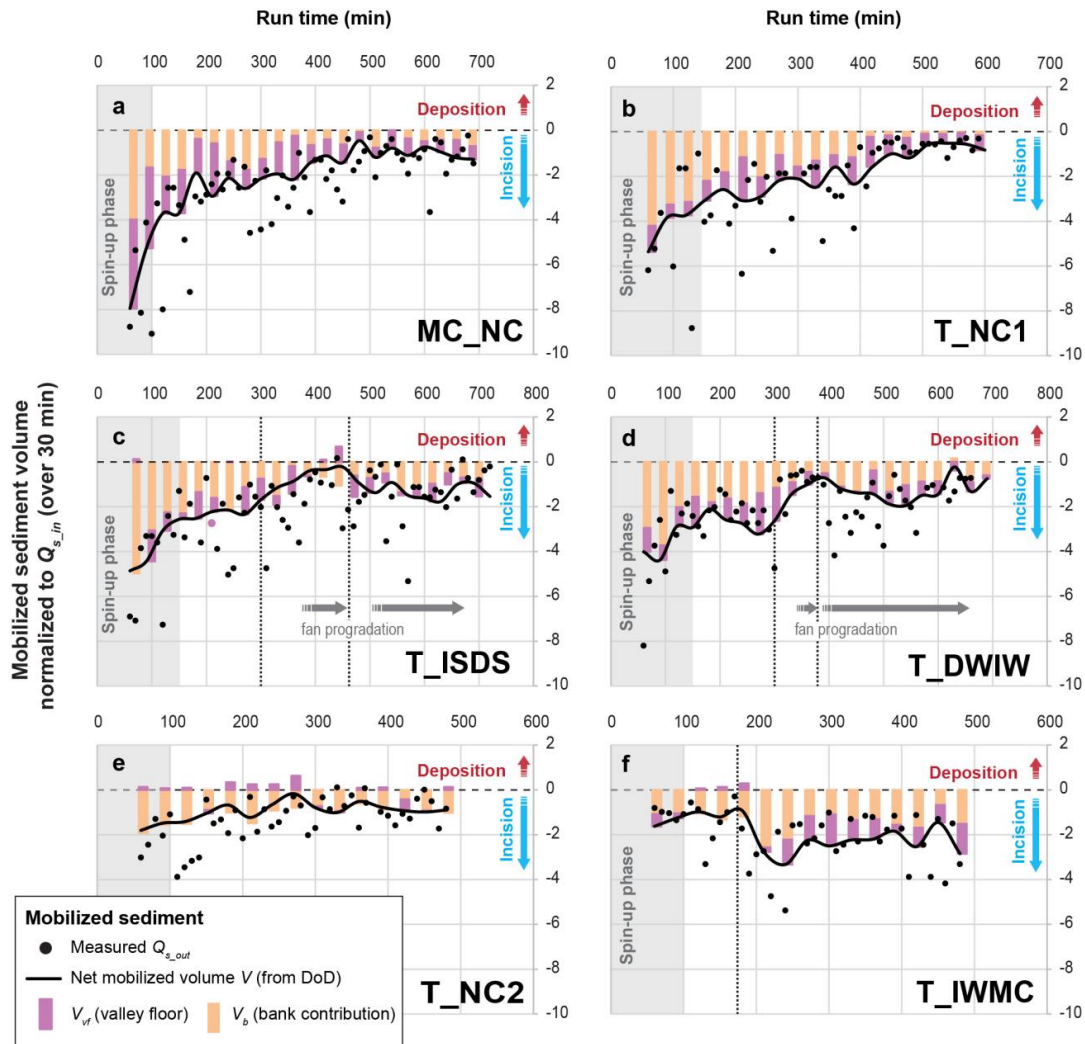
446 Our experiments offered a rare opportunity to evaluate the impacts of sediment supply from
447 the tributary to the main channel through space and time. In general, sediment moved in pulses,
448 and areas of deposition and incision commonly coexisted (Fig. 8a).

449 $Q_{s,out}$ varied greatly, but generally decreased through time (the only exception is the
450 T_IWMC run, where $Q_{s,out}$ remained high) (Fig. 8, black circles). Values for the mobilized
451 sediment, V , calculated from the DoDs (averaged over 30 minutes) show similar trends, but with
452 a lower variability that reflects the long-term average $Q_{s,out}$ (Fig. 8, black lines). An appreciable
453 reduction of $Q_{s,out}$ occurred when the system was approaching equilibrium (e.g., end of Fig. 8a,
454 b) and during times of fan aggradation in the tributary (i.e., IS and DW phases of Fig. 8c, d, and
455 e). Net mobilized sediment volumes (V) increased again during phases of fan incision (i.e., DS
456 and IW phases of Fig. 8c and d) and main-channel incision (e.g., IW phase in Fig. 8f). These
457 increases were due to the combined effect of a general increase in sediment mobility within the
458 active valley floor (V_{vf}) and lateral erosion of the banks (V_b) (Fig. 8, violet and orange bars
459 respectively, and Fig. S6 of the Supp. Material). The DoD analysis also indicates that in all
460 experiments, with the only exception of the MC run and of the phases approaching steady-state,
461 bank contribution was higher or of the same order of magnitude of the volume mobilized in the
462 valley floor (Fig. 8, orange and violet bars). This suggests that bank erosion represented a major
463 contribution to $Q_{s,out}$ (Tables S3 to S8 of Supp. Material). This is particularly true also for the



464 T_NC2 run, where aggradation was favored, in which Q_{s_out} is dominated by the contribution of
 465 the banks (Fig. 8e, and Fig. S7 of the Supp. Material).

466



467

468 Figure 8. Volumes of sediment mobilized within the system. Black line: Net mobilized volume
 469 of sediment measured using the DoD. For comparison, black dots represent the Q_{s_out} values
 470 measured every 10 minutes (part of the difference between measured and calculated Q_{s_out} values
 471 may be due to the contribution of the most downstream area of the wooden box, which was
 472 shielded in the DEM reconstruction). Horizontal arrows indicate the timespan of fan
 473 progradation either during fan aggradation or fan incision. Vertical pointed lines represent the
 474 *time of change* in boundary conditions; horizontal dashed line separates aggradation and erosion.



475

476 4.3. Downstream sediment propagation

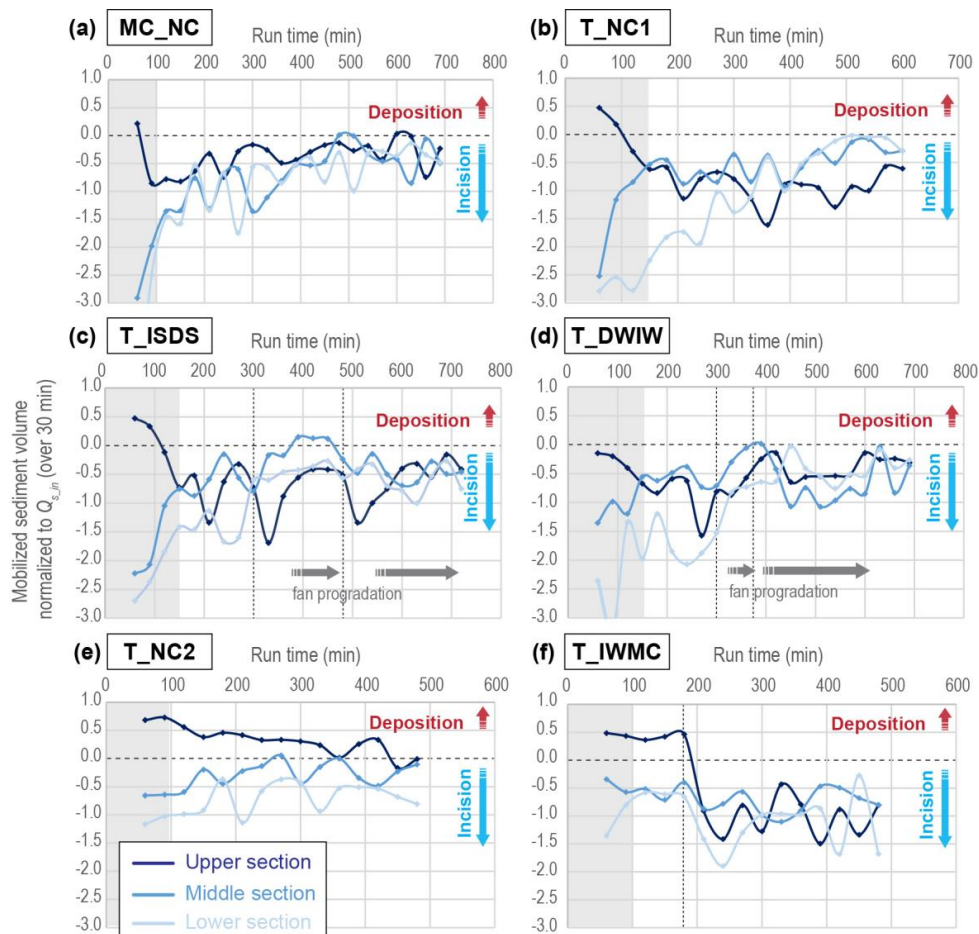
477 To analyze the effects of the tributary on the mobility of sediment within the coupled
478 tributary–main-channel system, we monitored the volumes of sediment mobilized (V) in the
479 upper, middle, and lower sections of the fluvial network through time (Fig. 9). The complex
480 pattern of V in the different sections yields insights into downstream sediment propagation,
481 especially when coupled with maps of the spatial distribution of eroded and deposited sediment
482 (Fig. 10, and Figs. S1 to S5 in the Supp. Material):

- 483 1. In all experiments, including the one without a tributary (MC_NC), sediment moved in
484 pulses through the system (Fig. 9). As such, the mobilized volumes (V) of each section
485 can be *in-phase* or *out-of-phase* with the volumes mobilized in the others sections
486 (Castelltort and Van Den Driessche, 2003) depending on where the “pulse” of sediment
487 was located within the floodplain (Fig. 11a).
- 488 2. The sediment mobilized in the middle and lower sections of the T_NC1 run showed a
489 decrease in V after ca. 400 min, whereas in the upper section V remained nearly constant
490 (Fig. 9b), despite a marked increase in V_{vf} (Fig. S6 of Supp. Material).
- 491 3. In the T_ISDS run, the middle section showed, as expected, a strong reduction in V after
492 the onset of increased $Q_{s,in}$ in the tributary and consequent fan aggradation (300 to 480
493 minutes). Conversely, it showed an increase in V following the decrease in $Q_{s,in}$ and
494 consequent fan incision (480 minutes to the end of the run) (Fig. 9c). A similar pattern
495 can be seen in the lower section, with a reduction in V during fan aggradation and an
496 increase in V during fan incision. Interestingly, the upper section showed two peaks of
497 enhanced V (i.e., increase in sediment export) just after the changes in the tributary,
498 followed by a prolonged reduction of V (i.e., decrease in sediment export) during phases
499 of fan progradation.
- 500 4. Patterns similar to those described for the T_ISDS can be seen for the T_DWIW run.
501 However, due to the type of change in the tributary (i.e., decrease in Q_w , which increases
502 the Q_s/Q_w ratio, reducing the sediment-transport capacity) and due to the shorter duration
503 of the perturbation (300 to 375 minutes), the first peak of enhanced V in the upper
504 section was barely visible, whereas the second peak was not present. Rather, the upper



- 505 section shows a continuous decrease in V until ca. 420 min, i.e., circa 45 minutes after
 506 the onset of increased Q_w in the tributary (Fig. 9d and Fig. S3 of Supp. Material).
 507 5. The T_NC2 experiment is dominated by aggradation and V values are rather constant;
 508 (Fig. 9e and Fig. S4 of Supp. Material). Similar to the final part of the T_NC1 run, the
 509 upper section of the main channel showed a general increasing trend in V_{vf} (Fig. S7 of
 510 Supp. Material).
 511 6. In the T_IWMC experiment, as expected, V increased immediately after the increase in
 512 Q_w in main channel in all three sections (indicating major incision), but was particularly
 513 evident in the upper and lower sections of the main channel (Fig. 9f).

514

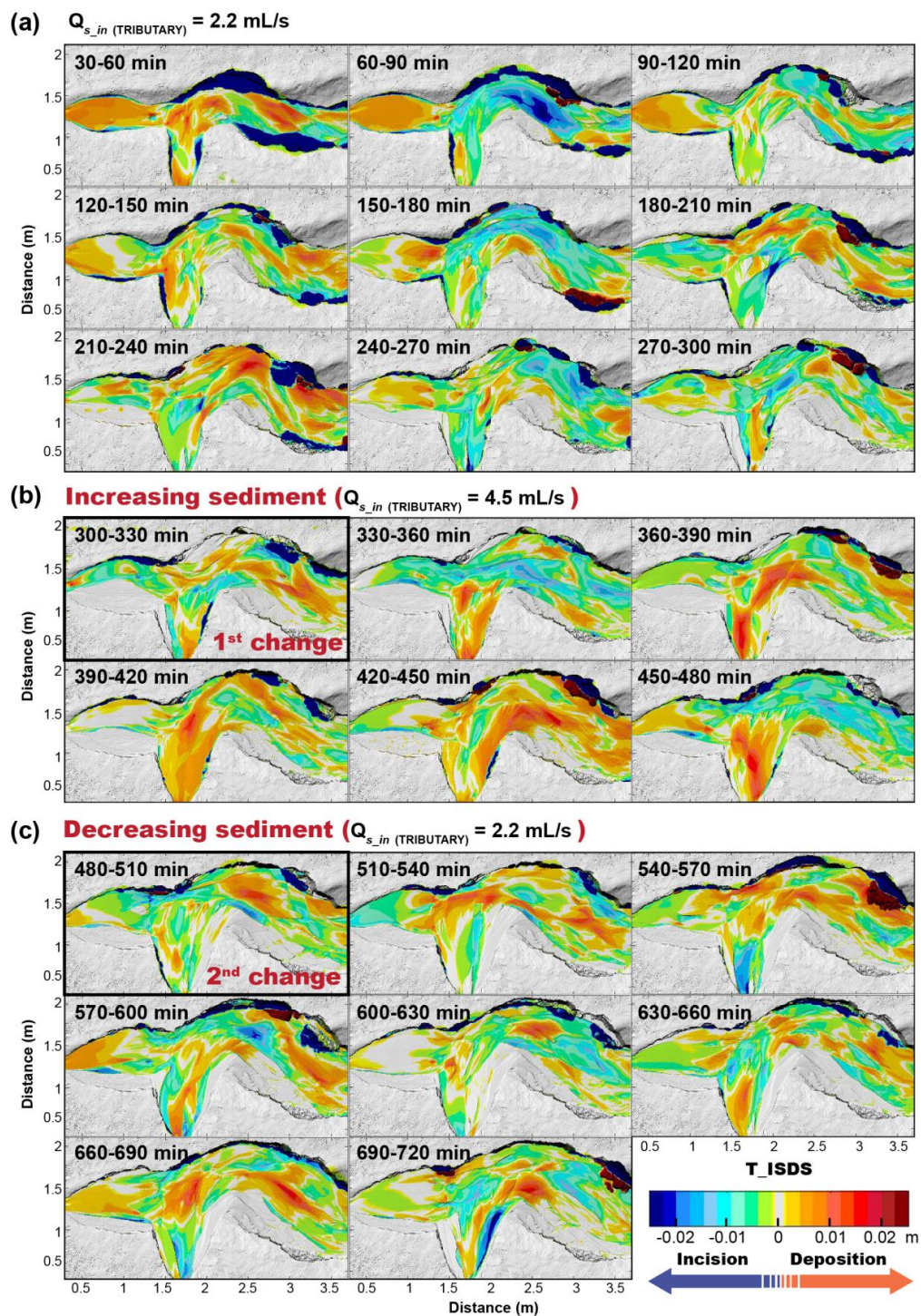


515



516 Figure 9. Volume (V) of sediment mobilized in each section (e.g., upper, middle, and lower
517 sections). Vertical lines represent the *times of change* in boundary conditions; horizontal dashed
518 line separates aggradation and erosion.

519





521 Figure 10. Sediment transfer dynamics within the system in the T_ISDS experiment (from DoDs
522 analysis). Variations between -0.001 and +0.001 m are considered as “no change” (in gray) to
523 account for the DEMs accuracy (i.e., 1 mm resolution). (a) Pre-perturbation phase (between 30
524 and 150 minutes is considered to be the spin-up phase); (b) Fan aggradation (300-390 min) and
525 progradation (390-480 min) phase; (c) Fan incision and progradation phase (480 min until end of
526 run).

527

528 5. Discussion

529 Our six experiments provide a conceptual framework for better understanding how tributaries
530 interact with main channels under different environmental forcing conditions (Fig. 1). We
531 particularly considered geometric variations of the two subsystems (i.e., tributaries and main
532 channels) and the effects of tributaries on the downstream delivery of sediment within the fluvial
533 system.

534 5.1. Aggrading and incising fans: geometrical adjustments and tributary–main- 535 channel interactions

536 In our experiments, the aggrading alluvial fans strongly impacted the width of the main-
537 channel valley both upstream and downstream of the tributary junction. By forcing the main
538 channel to flow against the valley-wall opposite the tributary, bank erosion was enhanced, thus
539 widening the main-channel valley floor (Figs. 4, 7, and 10). Bank erosion and valley widening in
540 the main channel also occurred during periods of fan incision (Figs. 10b, S3, and S6 of the Supp.
541 Material). We hypothesize that this widening was related to pulses of sediment eroded from the
542 fan, which periodically increased the sediment load to the main channel and helped to push the
543 river to the side opposite the tributary (Grimaud et al., 2017; Leeder and Mack, 2001). Once
544 there, the river undercut the banks, causing instability and collapse. As such, periods of fan
545 incision triggered a positive feedback between increased load in the main channel and valley
546 widening, which occurred mainly through bank erosion and bank collapses. In these scenarios,
547 bank contribution (V_b) in the middle and lower sections of the main channel can be equal to, or
548 larger than, the sediment mobilized within the active valley floor (V_{vf}) (also for the T_NC2 run;
549 Fig. 8b and Fig. S6 and S7, Supp. Material). It follows that the composition of the fluvial
550 sediment may be largely dominated by material mobilized from the valley walls, with important
551 consequences, for example, for geochemical or provenance studies (Belmont et al., 2011).



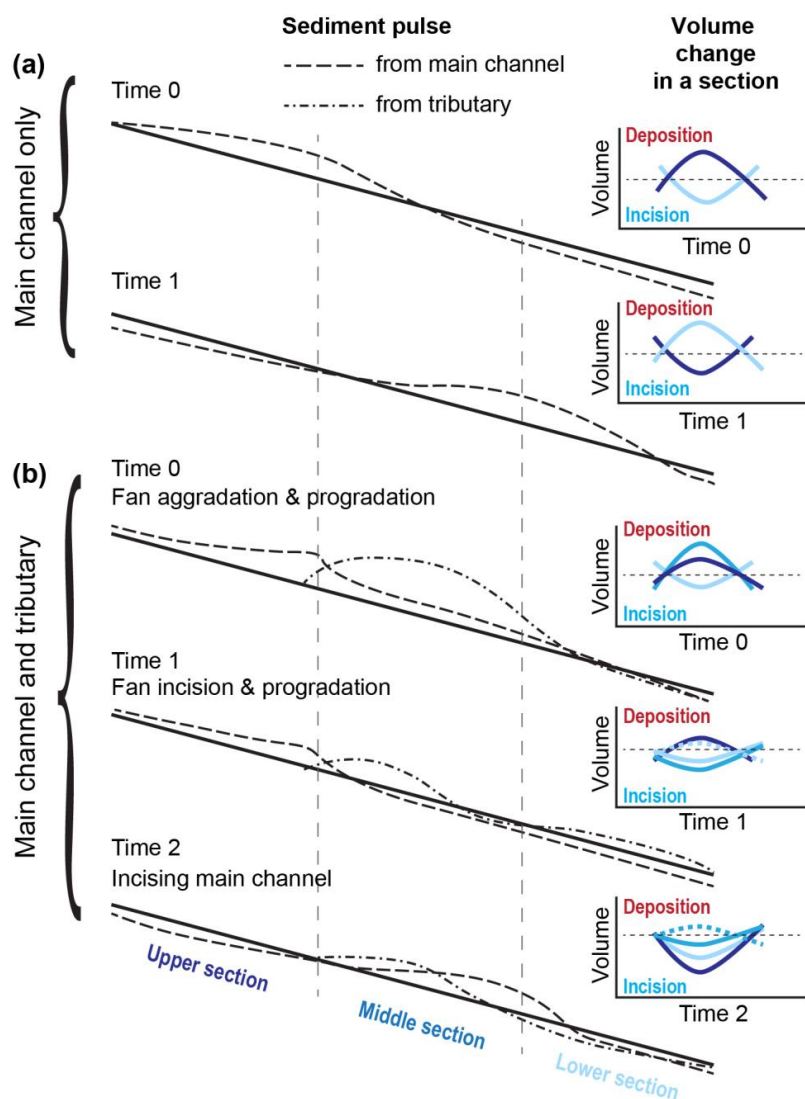
552 Our analysis of sediment mobility within the different sections of the main channel
553 highlighted that the presence of the alluvial fan affects the time needed to reach equilibrium in
554 the different reaches of the main river: in the T_NC1 run, for example, due to the sediment input
555 from the tributary, the middle and lower sections have a higher Q_s/Q_w ratio (0.022) than the
556 upper section (0.014), and may reach equilibrium faster (Gilbert, 1877; Wickert and Schildgen,
557 2019). Once the tributary reached equilibrium (e.g., at ca. 420 minutes for T_NC1; inset of Fig.
558 4b), the upper main channel rapidly adjusted by decreasing the elevation of its channel bed (Fig.
559 4b) and increasing the sediment mobilized (Fig. 9b and Fig. S6 of Supp. Material). This result
560 suggests that equilibrium time scales of channels upstream and downstream of tributaries can
561 vary (Schumm, 1973), and that in a top-down direction of adjustments, the equilibrium state of
562 the upper section may be dictated by the equilibrium state of its lower reaches because of the
563 tributary influence.

564 In our experiments, fans were built under conditions that caused deposition at the tributary
565 junction (e.g., an increase in Q_{s_in} or decrease in Q_w in the tributary). When the perturbation
566 lasted long enough (e.g. in experiment T_ISDS), the fan prograded into the main channel. The
567 passage from fan aggradation to progradation was delayed relative to the onset of the
568 perturbation by the time necessary to move the sediment from the fan head to the fan margin
569 (e.g. for > 60 min in T_ISDS; Fig. 10b). This delay allowed for a temporarily efficient transfer of
570 sediment within the main channel (as marked by the peak in V of the upper main channel section;
571 Fig. 9c). For tributaries subject to a change that caused tributary incision (e.g., decrease in Q_{s_in}
572 or increase in Q_w), the elevation of the fan surface was progressively lowered (inset of Fig. 4c
573 and d, and Fig. 6), and the fan prograded into the main channel with cyclic pulses of sediment
574 discharge (e.g., Fig. 10c) (Kim and Jerolmack, 2008). Progradation was generally localized
575 where the tributary channel debouched into the main river (e.g., depositing the *healing wedge* of
576 Leeder and Mack, 2001), generally shortly after (< 30 min) the onset of the perturbation (Figs.
577 10c and S3 of the Supp. Material). When the fan prograded, sediment in the main channel was
578 blocked above the tributary junction (e.g., at 390 to 480 min in Fig 10b, and at 510 min to the
579 end of the run in Fig.10c; Fig. S4 of Supp. Material), and the upstream main-channel section
580 experienced a prolonged decrease in sediment mobility due to localized aggradation (Fig. 9c and
581 d, and Fig. 11b).



582 Given the relative size of the tributary and main channel in our experiments (Q_w tributary ~
583 $2/3 Q_w$ main channel) and the magnitude of the perturbations (doubling of $Q_{s,in}$ or halving of
584 Q_w), the impact of perturbations in the tributary on the sediment mobility (V) within the main
585 channel remained mostly within autogenic variability (Fig. 8b, Group 1). This observation
586 highlights how the analysis of changes in $Q_{s,out}$ alone (for example inferred from the stratigraphy
587 of a fluvial deposit) may not directly reflect changes that occurred in the tributary, but can be
588 overprinted by autogenic variability. However, the analysis of V within individual sections of the
589 main channel, and particularly within the confluence zone (i.e., middle section), together with the
590 analysis of how sediment moves in space, reveal important changes in the sediment dynamics of
591 the main channel that may help to reconstruct the perturbations that affected the tributary
592 (Section 5.2; Figs. 9 and 11b). This observation underscores the need to study both the tributary
593 and main-channel deposits (Mather et al., 2017), both upstream and downstream of a tributary
594 junction.

595



596

597 Figure 11. Schematic representation of the average sediment mobilized in each section of the
 598 main channel. Solid black line represents the idealized equilibrium profile of the main channel,
 599 whereas dashed lines represent the volumes mobilized from the main channel and from the
 600 tributary. (a) Sediment dynamics in a single-channel system: sediment moves in pulses and upper
 601 and lower sections may be *out-of-phase* or *in-phase* depending on the dynamics of the middle
 602 section (i.e., the *transfer zone* of Castellort and Van Den Driessche, 2003). (b) Sediment
 603 dynamics in a tributary-main channel system: *Time 0* represents the “aggrading (and prograding)
 604 fan” scenario, where the upper and middle sections of the main channel undergo aggradation,
 605 while the lower section undergoes incision. *Time 1* represents the “incising (and prograding) fan”
 606 scenario, where the upper section may still be aggrading by it also starts to get incise creating a
 607 pulse of sediment that reaches the lower section. The middle section clearly sees an increase in



608 incision due to the imposed perturbation, while the lower section may undergo incision or
609 aggradation depending on the amount of sediment delivered from the fan, from the upper section,
610 and from bank erosion. *Time 2* represents the “incising main channel” scenario, where the fan
611 loses its influence on the dynamics of the main channel and both upper and lower sections
612 undergo incision. The middle section can undergo aggradation or incision depending on the
613 amount of sediment mobilized in the tributary and on the pulse of sediment moving from the
614 upper to the lower section of the main channel.

615

616 5.2. Incising main channel: geometric adjustments and tributary–main-channel 617 interactions

618 The main-channel bed elevation dictates the local base level of the tributary, such that
619 variations in the main-channel long profile may cause aggradation or incision in the tributary
620 (Cohen and Brierly, 2000; Leeder and Mack, 2001; Mather et al., 2017). In our experiments,
621 lowering of the main-channel bed triggered tributary incision that started at the fan toe and
622 propagated upstream (insets in Fig. 4). Because tributary incision increases the volume of
623 sediment supplied to the main channel, a phase of fan progradation would be expected, similar to
624 the cases described above (and in the *complex response* of Schumm, 1973). However, in our
625 experiment (i.e., T_IWMC), progradation did not occur: instead, the fan was shortened (Fig. S5
626 Supp. Material). We hypothesize that the increased transport capacity of the main river resulted
627 in an efficient removal of the additional sediment from the tributary, thereby mitigating the
628 impact of the increased sediment load supplied by the tributary to the main channel. Another
629 consequence is that the healing wedge of sediment from the tributary is likely not preserved in
630 the deposits of either the fan margin or the confluence zone, hindering the possibility to
631 reconstruct the changes affecting the tributary. However, some insight can be obtained from the
632 analysis of sediment mobility. During main-channel incision, whereas both upper and lower
633 sections of the main channel registered a marked increase in V following the perturbation, the
634 middle section showed only minor variations (Fig. 9f). We hypothesize that this lower variability
635 was due to the buffering effect of the increased load supplied from the fan undergoing incision
636 (i.e., caused by the sudden base-level fall that followed main-channel incision) (Fig. 11b). In
637 contrast, when incision in the tributary was caused by a perturbation in its headwaters, V initially
638 increased and then showed a prolonged decrease in the upper section during fan aggradation,
639 whereas it increased in the middle section during fan incision. These differences may help to



640 discern the cause of fan incision (i.e., either a perturbation in the main channel or in the
641 tributary).

642 We did not observe the *complex response* described by Schumm (1973), characterized by
643 tributary aggradation following incision along the main channel. That complex response likely
644 occurred because the main river had insufficient power to remove the sediment supplied by the
645 tributaries, as opposed to what occurred in our experiments. When aggradation occurs at the
646 tributary junction, one may expect to temporarily see an evolution similar to that proposed in the
647 “aggrading alluvial fan” scenario, with the development on an alluvial fan that may alter the
648 sediment dynamics of the main channel, modulating the sediment mobilized in the upper and
649 lower sections of the river and delaying main-channel adjustments. In our experiment, instead, a
650 prolonged erosional regime within the main channel may have led to fan entrenchment and fan-
651 surface abandonment (Clarke et al., 2008; Nicholas and Quine, 2007; Pepin et al., 2010; Van
652 Dijk et al., 2012). Despite the lack of fan progradation, an increase in bank contribution
653 following incision of the main channel did occur (Fig. 8b.6, Fig. S7 Supp. Material) and could be
654 explained by (1) higher and more unstable banks and (2) an increased capacity of the main
655 channel to laterally rework sediment volumes under higher water discharges (Bufe et al., 2019).

656 5.3. Sediment propagation and coupling conditions

657 Understanding the interactions between tributaries and main channel, and the contribution of
658 these two sub-system to the sediment moved (either eroded or deposited) in the fluvial system, is
659 extremely important for a correct interpretation of fluvial deposits (e.g., cut-and-fill terraces or
660 alluvial fans), which are often used to reconstruct the climatic or tectonic history of a certain
661 region (e.g., Armitage et al., 2011; Densmore et al., 2007; Rohais et al., 2012).

662 In their conceptual model, Mather et al. (2017) indicate that an alluvial fan may act as a
663 *buffer* for sediment derived from hillslopes during times of fan aggradation, and as a *coupler*
664 during times of fan incision, thereby allowing the tributary’s sedimentary signals to be
665 transmitted to the main channel. From our experiments, we can explore the effects that tributaries
666 have not only in storing or releasing sediment to the main channel, but also in modulating the
667 flux of sediment within the fluvial system. In doing so, we create a new conceptual framework
668 that takes into account the connectivity within a coupled alluvial fan-main channel system and



669 the mechanisms with which sediment and sedimentary signals may be recorded in local deposits
670 (Fig. 12). Results are summarized as follows:

671 *5.3.1. Aggrading and incising fans*

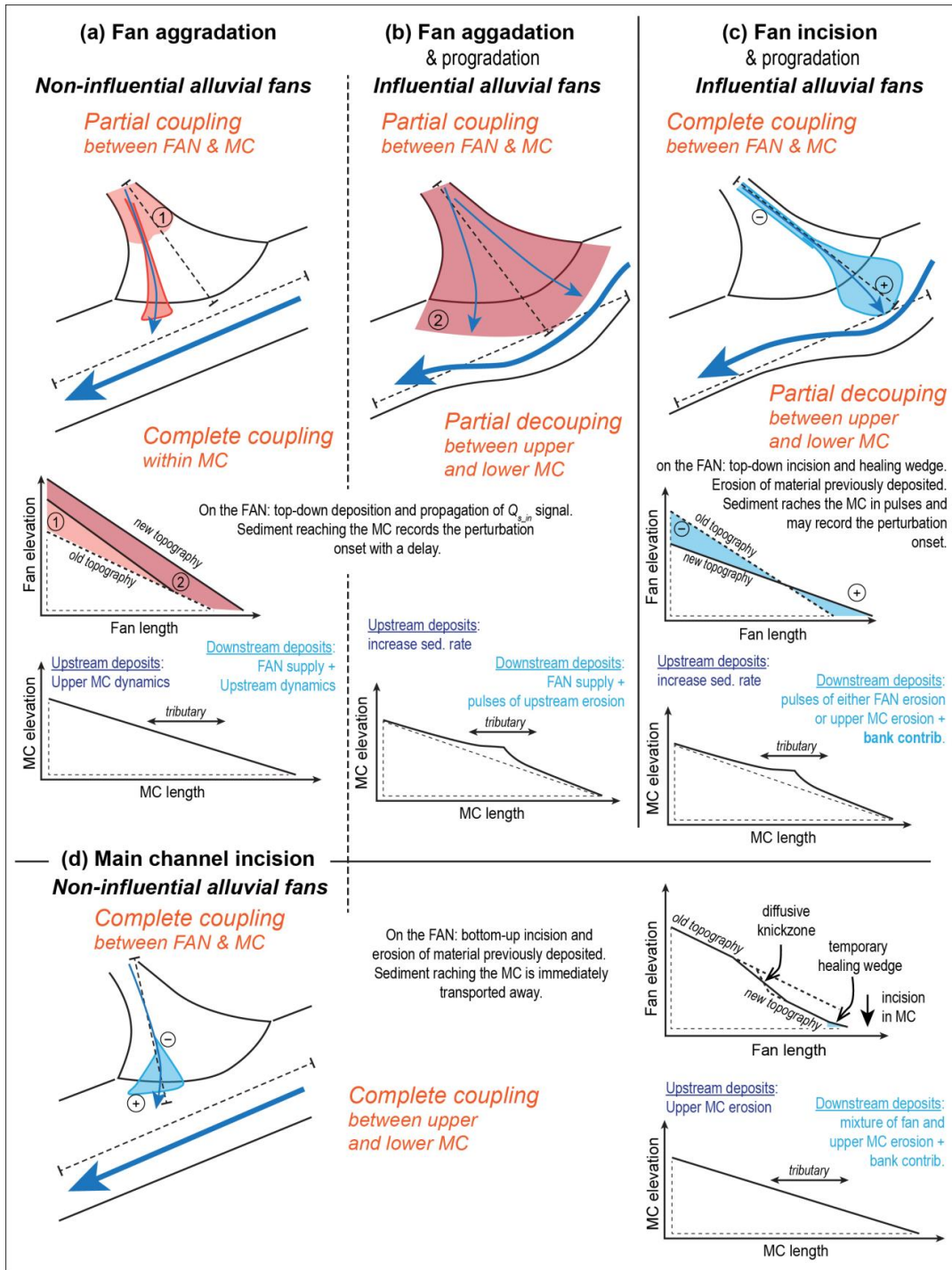
- 672 1. If the tributary has perennial water discharge, a *partial coupling* between the tributary
673 and the main channel is possible. Also, during fan aggradation, when most of the
674 sediment is deposited and stored within the fan (e.g., Fig 10b), a portion of the $Q_{s,in}$
675 reaches the main channel in proportion to the transport capacity of the tributary channel
676 (Fig. 12a and b). The partial coupling between the fan and the main channel allows for a
677 *complete coupling* between the upstream and downstream sections of the main river (Fig.
678 10b – 300-390 min, and S3b in the Supp. Material). As such, during fan aggradation, the
679 main channel behaves as a single connected segment, and the lower section receives
680 sediment in proportion to the transport capacity of the main and tributary channels. The
681 material supplied by the tributary to the main channel is dominated by the tributary's
682 $Q_{s,in}$ with little remobilization of previously deposited material.
- 683 2. During fan incision, large volumes of sediment are eroded from the fan and transported
684 into the main channel as healing wedges, allowing the fan to progade into the main
685 channel (Fig. 10c and 12c). This process creates a *complete coupling* between the
686 tributary and the main channel (Fig. 9c and d), with the material supplied by the tributary
687 mostly dominated by sediment previously deposited within the fan.
- 688 3. During times of fan progradation, the fan creates an obstacle to the transfer of sediment
689 down the main channel, creating a *partial decoupling* between upstream and downstream
690 sections of the main channel (Fig. 9, 10b and c, and 12b and c). As a consequence, the
691 sediment carried by the main channel is trapped above the tributary junction and thus will
692 be missing from downstream sedimentary deposits. However, the upstream section of the
693 main channel may be periodically subject to incision (e.g., Fig. 10b and c), moving
694 mobilized sediment from the upper to the lower section. Accordingly, if progradation of
695 the fan is due to prolonged fan aggradation, the downstream section will receive the $Q_{s,in}$
696 from the fan, plus pulses of sediment eroded from the upstream section of the main
697 channel. Conversely, if progradation is due to incision of the tributary and mobilization
698 of additional fan sediment, the downstream section will receive pulses of erosion from



699 either the fan or the upstream section of the main channel, plus the contribution of bank
700 erosion.

701 In summary, downstream fluvial deposits record the competition between the main
702 channel and the tributary: the alluvial fan pushes the main channel towards the opposite side
703 of the valley to adjust its length, whereas the main channel tries to maintain a straight course
704 by removing the material deposited from the fan. If the main channel dominates, it cuts the
705 fan toe and permits sediment from upstream of the junction to be more easily moved
706 downstream. If the tributary dominates, the main channel will be displaced and the transfer of
707 sediment through the junction will be disrupted. An autogenic alternation of these two
708 situations is possible, whereby fan-toe cutting may trigger fan incision and progradation,
709 increasing the influence of the fan on the main channel. The composition of the sediment
710 downstream thus reflects the competition between main channel and alluvial fan, with
711 contributions from both sub-catchments. In addition, bank erosion may make important
712 contributions to sediment supply and transport, particularly during periods of fan incision
713 (Fig. S6 in the Supp. Material). From these results, we therefore distinguish between: 1)
714 *Influential alluvial fans*, which have a strong impact on the geometry and sediment-transfer
715 dynamics of the main channel, and 2) *Non-influential alluvial fans*, which do not
716 substantially alter the geometry or sediment-transfer dynamics of the main channel.

717





719 Figure 12. Conceptual framework for the coupling conditions of an alluvial-fan/main-channel
720 (MC) system under different environmental forcings. For *aggrading and incising alluvial fans*
721 (upper panels), the fan-main channel connectivity depends on the dynamics acting in the alluvial
722 fan, being partially coupled during fan aggradation and totally coupled during fan incision. For
723 *incising main rivers* (lower panel) the fan and main channel are fully coupled. As well, *non-*
724 *influential alluvial fans* (left and lower panels) favors a complete coupling within the main
725 channel, whereas *influential alluvial fans* (middle and right upper panels) may favor a partial
726 decoupling between upstream and downstream sections of the main river. Each one of the four
727 settings presented here brings its own sedimentary signature, different responses to perturbations,
728 and dynamics of signal propagation which may be recorded into the fluvial deposits.

729

730 5.3.2. *Incising main channel*

- 731 1. Lowering of the main-channel bed triggers incision into the alluvial fan, thereby
732 promoting a *complete coupling* between the fan and the main channel (Fig. 12d, and S5
733 in the Supp. Material). The sediment supplied by the tributary is mainly composed of
734 material previously deposited within the fan.
- 735 2. An increase in main-channel water discharge increases the transport capacity of the
736 mainstem so that it persistently “wins” the competition with the alluvial fan. In this case,
737 despite the incision triggered in the alluvial fan, which increases the sediment supplied by
738 the tributary, the main channel efficiently removes the additional sediment load, thereby
739 reducing the influence of the alluvial fan on downstream sediment transport within the
740 main channel (Fig.S5 in the Supp. Material). The consequence is a *complete coupling*
741 between the upstream and downstream sections of the main channel (Fig. 12d). The
742 sediment reaching the lower section is a mixture of eroded material from the main
743 channel, within the fan, and along the banks.

744 6. Conclusion

745 We performed six experiments to analyze the interactions of a tributary–main-channel
746 system when a tributary produces an alluvial fan. We found that differing degrees of coupling
747 may be responsible for substantial changes in the geometry of the main channel and the sediment
748 transfer dynamics of the system. In general, we found that the channel geometry (i.e., channel
749 slope and valley width) adjusts to changes in sediment and water discharge in accordance with
750 theoretical models (e.g., Ferguson and Hoey, 2008; Parker et al., 1998; Whipple et al., 1998;
751 Wickert and Schildgen, 2019). Additionally, by analyzing the effects of the tributary-main



752 channel interactions on the downstream delivery of sediment, we have shown that the fluvial
753 deposits within the main channel above and below the tributary junction may record
754 perturbations to the environmental conditions that govern the fluvial system.

755 Our main results can be summarized as follows (Fig. 12):

756 (1) Fan aggradation leads to a partial coupling between the fan and the main channel, which
757 permits a complete coupling between the main-channel reaches upstream and downstream of the
758 tributary junction. As such, the provenance of downstream sediment reflects the dynamics of
759 both sub-catchments (e.g., tributary and main river), and remobilized material from older
760 deposits will be minimal.

761 (2) Fan incision favors a complete coupling between the fan and the main channel, and
762 remobilizes material previously stored in the fan.

763 (3) Fan progradation (either during prolonged aggradation or fan incision) strongly
764 influences the main channel. As a result, the connectivity of the main river across the tributary
765 junction is reduced and the deposits of the fluvial system above and below the junction may
766 record different processes.

767 (4) Incision along the main channel triggers incision in the alluvial fan that, despite an
768 increased sediment supply to the main river, reduces its influence on the dynamics of the main
769 channel. The result is a fully connected fluvial system in which the deposits record sediment-
770 transfer dynamics and the interactions between both the alluvial fan and the main river, including
771 a large component of material remobilized from older deposits.

772 The theoretical framework proposed in this study aims to illustrate the dynamics acting
773 within a tributary junction, which is an ubiquitous phenomenon across many environments. It
774 provides a first-order analysis of how tributaries affect the sediment delivered to the main
775 channels, and of how sediment is moved through the system under different environmental
776 forcing conditions. With this information we hope to provide a better understanding of the
777 composition and architecture of fluvial sedimentary deposits found at confluence zones, which is
778 essential for a correct reconstruction of the climatic or tectonic histories of a basin.



779 **Data availability**

780 Data will be made available.

781 **Video supplement**

782 Time-lapse video of the experiment will be uploaded.

783 **Supplement**

784 Supplement tables and figures can be found in the supplementary document.

785 **Author contributions**

786 SS, ST, and ADW designed and built the experimental setup. SS and ST performed the
787 experiments. SS analyzed the data with the help of ST, ADW and AB. All authors discussed the
788 data, designed the manuscript, and commented on it. SS designed the artwork.

789

790 **Competing interests**

791 The authors declare that they have no conflict of interest.

792

793 **Acknowledgments**

794 We thank Ben Erickson, Richard Christopher, Chris Ellis, Jim Mullin, and Eric Steen for
795 their help in building the experimental setup and installing equipment. We are also thankful to
796 Jean-Louis Grimaud and Chris Paola for fruitful discussions and suggestions.

797

798 **Financial support**

799 This research has been supported by the Deutsche Forschungsgemeinschaft (grant no. SCHI
800 1241/1-1 and grant no. SA 3360/2-1), the Alexander von Humboldt-Stiftung (grant no. ITA
801 1154030 STP), and the University of Minnesota.

802

803 **References**

804 Allen, P. A.: From landscapes into geological history, *Nature*, 451, 274–276,
805 <https://doi.org/10.1038/nature06586>, 2008.



- 806
807 Armitage, J. J., Duller, R. A., Whittaker, A. C., and Allen, P. A.: Transformation of tectonic
808 and climatic signals from source to sedimentary archive, *Nat. Geosci.*, 4, 231–235, 2011.
809
- 810 Belmont, P., Gran, K.B., Schottler, S.P., Wilcock, P.R., Day, S.S., Jennings, C., Lauer, J.W.,
811 Viparelli, E., Willenbring, J.K., Engstrom, D.R., and Parker, G.: Large Shift in Source of Fine
812 Sediment in the Upper Mississippi River. *Environmental Science and Technology*, 45, 8804–
813 8810, 2011.
814
- 815 Benda, L.: Confluence environments at the scale of river networks. In: *River Confluences,*
816 *Tributaries and the Fluvial Network* © John Wiley & Sons, Ltd. ISBN: 978-0-470-02672-4,
817 2008.
818
- 819 Benda, L., Miller, D., Bigelow, P., and Andras, K.: Effects of post-wildfire erosion on
820 channel environments, Boise River, Idaho. *Forest Ecology and Management*, v. 178, 105–119,
821 doi:10.1016/S0378-1127(03)00056-2, 2003.
822
- 823 Benda, L., Leroy Poff, N., Miller, D., Dunne, T., Reeves, G., Pess, G., and Pollock, M.: The
824 Network Dynamics Hypothesis: How Channel Networks Structure Riverine Habitats.
825 *BioScience*, v. 54(5), 413-427, 2004a.
826
- 827 Benda, L., Andras, K., Miller, D., and Bigelow, P.: Confluence effects in rivers: Interactions
828 of basin scale, network geometry, and disturbance regime. *Water Resources Research*, 40,
829 W05402, doi:10.1029/2003WR002583, 2004b.
830
- 831 Best, J.L.: The morphology of river channel confluences. *Progress in Physical Geography:*
832 *Earth and Environment*, v. 10(2), 157-174, <https://doi.org/10.1177/030913338601000201>, 1986.
833
- 834 Best, J.L.: Sediment transport and bed morphology at river channel confluences.
835 *Sedimentology*, 35,481-498, 1988.
836
- 837 Best, J.L., and Rhoads B.L.: Sediment transport, bed morphology and the sedimentology of
838 river channel
839 Confluences. In: *River Confluences, Tributaries and the Fluvial Network* © John Wiley &
840 Sons, Ltd. ISBN: 978-0-470-02672-4, 2008.
841
- 842 Bierman, P. and Steig, E. J.: Estimating rates of denudation using cosmogenic isotope
843 abundances in sediment, *Earth Surf. Proc. Land.*, 21, 125–139,
844 [https://doi.org/10.1002/\(SICI\)1096-9837\(199602\)21:2<125::AID-ESP511>3.0.CO;2-8](https://doi.org/10.1002/(SICI)1096-9837(199602)21:2<125::AID-ESP511>3.0.CO;2-8), 1996.
845
- 846 Brown, E. T., Stallard, R. F., Larsen, M. C., Raisbeck, G. M., and Yiou, F.: Denudation rates
847 determined from the accumulation of in situ-produced ¹⁰Be in the Luquillo Experimental Forest,
848 Puerto Rico, *Earth Planet. Sc. Lett.*, 129, 193–202, [https://doi.org/10.1016/0012-](https://doi.org/10.1016/0012-821X(94)00249-X)
849 [821X\(94\)00249-X](https://doi.org/10.1016/0012-821X(94)00249-X), 1995.
850



- 851 Bryant M., Falk P., and Paola C.: Experimental study of avulsion frequency and rate of
852 deposition. *Geology*; v. 23; no. 4; 365–368, 1995.
853
- 854 Bufe, A., Turowski, J.M., Burbank, D.W., Paola, C., Wickert, A.D., and Tofelde, S.:
855 Controls on the lateral channel migration rate of braided channel systems in coarse non-cohesive
856 sediment. *Earth Surface Processes and Landforms*, <https://doi.org/10.1002/esp.4710>, 2019.
857
- 858 Bull W.B.: Threshold of critical power in streams. *Geological Society of America Bulletin*,
859 Part I, v. 90, 453-464, 1979.
860
- 861 Castelltort S., and Van Den Driessche J.: How plausible are high-frequency sediment
862 supply-driven cycles in the stratigraphic record? *Sedimentary Geology*, v. 157, 3–13;
863 doi:10.1016/S0037-0738(03)00066-6, 2003.
864
- 865 Clarke L. E., Quine T.A., and Nicholas A.P.: *Sediment Dynamics in Changing*
866 *Environments* (Proceedings of a symposium held in Christchurch, New Zealand, December
867 2008). IAHS Publ. 325, 2008.
868
- 869 Clarke L. E., Quine T.A., and Nicholas A.P.: An experimental investigation of autogenic
870 behaviour during alluvial fan evolution. *Geomorphology*, v. 115, 278–285;
871 doi:10.1016/j.geomorph.2009.06.033, 2010.
872
- 873 Cohen, T.J., and Brierley, G.J.: Channel instability in a forested catchment: a case study
874 from Jones Creek, East Gippsland, Australia. *Geomorphology*, 32, 109–128, 2000.
875
- 876 D'Arcy, M., Roda-Boluda, D.C., Whittaker, A.C.: Glacial-interglacial climate changes
877 recorded by debris flow fan deposits, Owens Valley, California. *Quaternary Science Reviews*,
878 169, 288-311, 2017.
879
- 880 Dingle, E. H., Attal, M., and Sinclair, H. D.: Abrasion-set limits on Himalayan gravel flux,
881 *Nature*, 544, 471–474, 5 <https://doi.org/10.1038/nature22039>, 2017.
882
- 883 De Haas T., Van den Berg W., Braat L., and Kleinhans M.G.: Autogenic avulsion,
884 channelization and backfilling dynamics of debris-flow fans. *Sedimentology*, v. 63, 1596–1619.
885 Doi; 10.1111/sed.12275, 2016.
886
- 887 Densmore A.L., Allen P.A., and Simpson G.: Development and response of a coupled
888 catchment fan system under changing tectonic and climatic forcing. *J. Geophys. Res.*, 112,
889 F01002, doi:10.1029/2006JF000474, 2007
890
- 891 Faulkner, D.J., Larson, P.H., Jol, H.M., Running, G.L., Loope, H.M., and Goble, R.J.:
892 Autogenic incision and terrace formation resulting from abrupt late-glacial base-level fall, lower
893 Chippewa River, Wisconsin, USA. *Geomorphology*, v. 266, 75–95,
894 <http://dx.doi.org/10.1016/j.geomorph.2016.04.016>, 2016.
895



- 896 Ferguson, R.I., Cudden, J.R., Hoey, T.B., and Rice, S.P.: River system discontinuities due to
897 lateral inputs: generic styles and controls. *Earth Surf. Process. Landforms*, v. 31, 1149–1166, doi:
898 10.1002/esp.1309, 2006.
- 899
900 Ferguson, R.I., and Hoey, T.: Effects of tributaries on main-channel geomorphology. In:
901 *River Confluences, Tributaries and the Fluvial Network* © John Wiley & Sons, Ltd. ISBN: 978-
902 0-470-02672-4, 2008.
- 903
904 Gao L., Wang X., Yi S., Vandenberghe J., Gibling M.R., and Lu H.: Episodic Sedimentary
905 Evolution of an Alluvial Fan (Huangshui Catchment, NE Tibetan Plateau). *Quaternary*, v. 1(16);
906 doi:10.3390/quat1020016, 2018.
- 907
908 Germanoski, D., Ritter, D.F.: Tributary response to local base level lowering below a dam.
909 *Regulated rivers: research and management*, v. 2, 11-24, 1988.
- 910
911 Gilbert, G. K.: Report on the Geology of the Henry Mountains, US Gov. Print. Off.,
912 Washington, D.C., USA, <https://doi.org/10.3133/70038096>, 1877.
- 913
914 Giles P.T., Whitehouse B.M., and Karymbalis E.: Interactions between alluvial fans and
915 axial rivers in
916 Yukon, Canada and Alaska, USA. From: Ventra, D. & Clarke, L. E. (eds) *Geology and
917 Geomorphology of Alluvial and Fluvial Fans: Terrestrial and Planetary Perspectives*. Geological
918 Society, London, Special Publications, v. 440; <http://doi.org/10.1144/SP440.3>, 2016.
- 919
920 Gippel, C.: Changes in stream channel morphology at tributary junctions, Lower Hunter
921 Valley,
922 New South Wales. *Australian GeOgQphiCQI Studies*, v. 23, 291-307, 1985.
- 923
924 Grant, G.E., and Swanson, F.J.: Morphology and Processes of Valley Floors in Mountain
925 Streams,
926 Western Cascades, Oregon. *Natural and Anthropogenic Influence in Fluvial
927 Geomorphology*, Geophysical Monograph, 89, 1995.
- 928
929 Granger, D. E., Kirchner, J. W., and Finkel, R.: Spatially averaged long-term erosion rates
930 measured from in situ-produced cosmogenic nuclides in alluvial sediment, *J. Geol.*, 104, 249–
931 257, 1996.
- 932
933 Heine, R.A., and Lant, C.L.: Spatial and Temporal Patterns of Stream Channel Incision in
934 the Loess Region of the Missouri River, *Annals of the Association of American Geographers*,
935 99(2), 231-253, DOI: 10.1080/00045600802685903, 2009.
- 936
937 Hamilton P.B., Strom K., and Hoyal D.C.J.D.: Autogenic incision-backfilling cycles and
938 lobe formation during the growth of alluvial fans with supercritical distributaries.
939 *Sedimentology*, v. 60, 1498–1525; doi: 10.1111/sed.12046, 2013.
- 940



- 941 Hooke R.L.: Model Geology: Prototype and Laboratory Streams: Discussion. Geological
942 Society of America Bulletin, v. 79, 391-394, 1968.
943
- 944 Hooke R.L., and Rohrer W.L.: Geometry of alluvial fans: effect of discharge and sediment
945 size. Earth Surface Processes, v. 4, 147-166, 1979.
946
- 947 Kim W., and Jerolmack D.J.: The Pulse of Calm Fan Deltas. The Journal of Geology, 11(4),
948 315-330; <http://dx.doi.org/10.1086/588830>, 2008.
949
- 950 Lane, E. W.: Importance of fluvial morphology in hydraulic engineering, Proceedings of the
951 American Society of Civil Engineers, 81, 1–17, 1955.
952
- 953 Larson P.H., Dorn R.I., Faulkner D.J., and Friend d.A.: Toe-cut terraces: A review and
954 proposed criteria to differentiate from traditional fluvial terraces. Progress in Physical
955 Geography, v. 39(4), 417–439, 2015.
956
- 957 Leeder M.R., and Mack G.H.: Lateral erosion (“toe-cutting”) of alluvial fans by axial rivers:
958 implications for basin analysis and architecture. Journal of the Geological Society, London, v.
959 158, 885-893, 2001.
960
- 961 Leopold, L.B., and Maddock, T. Jr.: The Hydraulic Geometry of Stream Channels and Some
962 Physiographic Implications. Geological survey professional paper 252, 1953.
963
- 964 Lupker, M., Blard, P., Lavé, J., France-Lanord, C., Leanni, L., Puchol, N., Charreau, J., and
965 Bourlès, D.: ¹⁰Be-derived Himalayan denudation rates and sediment budgets in the Ganga basin.
966 Earth and Planetary Science Letters, 333–334, 146–156, doi:
967 <http://dx.doi.org/10.1016/j.epsl.2012.04.020>, 2012.
968
- 969 Mackin J.H.: Concept of the graded river. Bulletin of the Geological Society of America, v.
970 69, 463-512, 1948.
971
- 972 Mather A.E., Stokes M., and Whitfield E.: River terraces and alluvial fans: The case for an
973 integrated Quaternary fluvial archive. Quaternary Science Reviews, v. 166, 74-90;
974 <http://dx.doi.org/10.1016/j.quascirev.2016.09.022>; 2017.
975
- 976 Meyer-Peter, E. and Müller, R.: Formulas for Bed-Load Transport, in: 2nd Meeting of the
977 International Association for Hydraulic Structures Research, 7–9 June 1948, Stockholm,
978 Sweden, International
979 Association for Hydraulic Structures Research, 39–64, 1948.
980
- 981 Miller, J.P.: High Mountain Streams: Effects of Geology on Channel Characteristics and
982 Bed Material. State bureau of mines and mineral resources New Mexico institute of mining and
983 technology Socorro, New Mexico. Memoir 4, 1958.
984
- 985 Mouchéné, M., van der Beek, P., Carretier, S., and Mouthereau, F.: Autogenic versus
986 allogenic controls on the evolution of a coupled fluvial megafan–mountainous catchment system:



- 987 numerical modelling and comparison with the Lannemezan megafan system (northern Pyrenees,
988 France). *Earth Surf. Dynam.*, 5, 125–143, doi:10.5194/esurf-5-125-2017, 2017.
989
- 990 Nicholas, A.P., Quine, T.A.: Modeling alluvial landform change in the absence of external
991 environmental forcing. *Geology*, v. 35(6), 527–530; doi: 10.1130/G23377A.1, 2007.
992
- 993 Nicholas, A. P., Clarke L., and Quine T. A.: A numerical modelling and experimental study
994 of flow width dynamics on alluvial fans. *Earth Surf. Process. Landforms* 34, 1985–1993;
995 DOI: 10.1002/esp.1839;, 2009.
996
- 997 Paola, C., Straub, K., Mohrig, D., and Reinhardt L.: The “unreasonable effectiveness” of
998 stratigraphic and geomorphic experiments. *Earth-Science Reviews*, v. 97(1–4), 1-43,
999 <https://doi.org/10.1016/j.earscirev.2009.05.003>, 2009.
1000
- 1001 Parker, G.: Hydraulic geometry of active gravel rivers, *J. Hydraul. Div.*, 105, 1185–1201,
1002 1978.
1003
- 1004 Parker, G.: Progress in the modeling of alluvial fans, *Journal of Hydraulic Research*, 37(6),
1005 805-825, <http://dx.doi.org/10.1080/00221689909498513>, 1999.
1006
- 1007 Parker, G. Paola, C., Whipple, K.X., and Mohrig, D.: Alluvial fans formed by channelized
1008 fluvial
1009 And sheet flow. I: Theory. *Journal of Hydraulic Engineering*, v. 124(10), 1998.
1010
- 1011 Pepin, E., Carretier, S., and Herail, G.: Erosion dynamics modelling in a coupled catchment–
1012 fan system with constant external forcing. *Geomorphology*, v. 122, 78–90,
1013 doi:10.1016/j.geomorph.2010.04.029, 2010.
1014
- 1015 Reitz, M.D., Jerolmack, D.J., and Swenson J.B.: Flooding and flow path selection on
1016 alluvial fans and deltas. *Geophysical Research Letters*, v. 37, L06401,
1017 doi:10.1029/2009GL041985, 2010.
1018
- 1019 Reitz, M.D., and Jerolmack, D.J.: Experimental alluvial fan evolution: Channel dynamics,
1020 slope controls, and shoreline growth. *Geophysical Research Letters*, v. 117, F02021,
1021 doi:10.1029/2011JF002261, 2012.
1022
- 1023 Rice, S.P., and Church, M.: Longitudinal profiles in simple alluvial systems. *Water*
1024 *Resources Research*, v. 37(2), 417-426, 2001.
1025
- 1026 Rice, S.P., Kiffney, P., Greene, C., and Pess, G.R.: The ecological importance of tributaries
1027 and confluences. In: *River Confluences, Tributaries and the Fluvial Network* © John Wiley &
1028 Sons, Ltd. ISBN: 978-0-470-02672-4, 2008.
1029
- 1030 Ritter, J.B., Miller, J.R., Enzel, Y., and Wells, S.G.: Reconciling the roles of tectonism and
1031 climate in Quaternary alluvial fan evolution. *Geology*, v. 23(3), 245–248, 1995.
1032



- 1033 Rohais, S., Bonnet, S., and Eschard, R.: Sedimentary record of tectonic and climatic
1034 erosional perturbations in an experimental coupled catchment-fan system. *Basin Research*, v. 24,
1035 198–212, doi: 10.1111/j.1365-2117.2011.00520.x, 2012.
- 1036
1037 Savi, S., Norton, K. P., Picotti, V., Akçar, N., Delunel, R., Brardinoni, F., Kubik, P., and
1038 Schlunegger, F.: Quantifying sediment supply at the end of the last glaciation: Dynamic
1039 reconstruction of an alpine debris-flow fan, *GSA Bull.*, 126, 773–790,
1040 <https://doi.org/10.1130/B30849.1>, 2014.
- 1041
1042 Savi, S., Schildgen T. F., Tofelde S., Wittmann H., Scherler D., Mey J., Alonso R. N., and
1043 Strecker M. R.: Climatic controls on debris-flow activity and sediment aggradation: The Del
1044 Medio fan, NW Argentina, *J. Geophys. Res. Earth Surf.*, 121, 2424–2445,
1045 doi:10.1002/2016JF003912, 2016.
- 1046
1047 Schildgen, T. F., Robinson, R. A. J., Savi, S., Phillips, W. M., Spencer, J. Q. G., Bookhagen,
1048 B., Scherler, D., Tofelde, S., Alonso, R. N., Kubik, P. W., Binnie, S. A., and Strecker, M. R.:
1049 Landscape response to late Pleistocene climate change in NW Argentina: Sediment flux
1050 modulated by basin geometry and connectivity, *J. Geophys. Res.-Earth*, 121, 392–414,
1051 <https://doi.org/10.1002/2015JF003607>, 2016.
- 1052
1053 Schumm, S. A.: Geomorphic thresholds and complex response of drainage systems, *Fluv.*
1054 *Geomorphol.*, 6, 69–85, 1973.
- 1055
1056 Schumm, S. A. and Parker, R. S.: Implication of complex response of drainage systems for
1057 Quaternary alluvial stratigraphy, *Nat. Phys. Sci.*, 243, 99–100, 1973.
- 1058
1059 Schwanghart, W. and Scherler, D.: Short Communication: TopoToolbox 2 – MATLAB-
1060 based software for topographic analysis and modeling in Earth surface sciences, *Earth Surf.*
1061 *Dynam.*, 2, 1-7, <https://doi.org/10.5194/esurf-2-1-2014>, 2014.
- 1062
1063 Simon, A., and Rinaldi, M.: Channel instability in the loess area of the midwestern United
1064 States. *Journal of the American Water Resources Association*, v. 36(1), Paper No. 99012, 2000.
- 1065
1066 Straub, K.M., Paola, C., Mohrig, D., Wolinsky, M.A., and George, T.: Compensational
1067 stacking of channelized sedimentary deposits. *Journal of Sedimentary Research*, v. 79, 673–688,
1068 doi: 10.2110/jsr.2009.070, 2009.
- 1069
1070 Tofelde, S., Savi, S., Wickert, A. D., Bufe, A., and Schildgen, T. F.: Alluvial channel
1071 response to environmental perturbations: fill-terrace formation and sediment-signal disruption,
1072 *Earth Surf. Dynam.*, 7, 609-631, <https://doi.org/10.5194/esurf-7-609-2019>, 2019.
- 1073
1074 Van den Berg van Saparoea, A.P. H., and Postma, G.: Control of climate change on the yield
1075 of river systems, *Recent Adv. Model. Siliciclastic Shallow-Marine Stratigr. SEPM Spec. Publ.*,
1076 90, 15–
1077 33, 2008.
- 1078



- 1079 Van Dijk, M., Postma, G., and Kleinhans, M.G.: Autocyclic behaviour of fan deltas: an
1080 analogue experimental study. *Sedimentology*, v. 56, 1569–1589, doi: 10.1111/j.1365-
1081 3091.2008.01047.x, 2009.
- 1082
1083 Van Dijk, M., Kleinhans, M.G., Postma, G., and Kraal, E.: Contrasting morphodynamics in
1084 alluvial fans and fan deltas: effect of the downstream boundary. *Sedimentology*, v. 59, 2125–
1085 2145 doi: 10.1111/j.1365-3091.2012.01337.x, 2012.
- 1086
1087 Von Blanckenburg, F.: The control mechanisms of erosion and weathering at basin scale
1088 from cosmogenic nuclides in river sediment. *Earth and Planetary Science Letters*, v. 237, 462–
1089 479, 2005.
- 1090
1091 Whipple, K.X., Parker, G. Paola, C., and Mohrig, D.: Channel Dynamics, Sediment
1092 Transport, and the Slope of Alluvial Fans: Experimental Study. *The Journal of Geology*, v. 106,
1093 677–693, 1998.
- 1094
1095 Whipple, K.X., and Tucker, G.E.: Implications of sediment-flux-dependent river incision
1096 models for landscape evolution. *Journal of Geophysical Research*, 107, B2, 2039, doi:
1097 10.1029/2000JB000044, 2002.
- 1098
1099 Wickert, A. D. and Schildgen, T. F.: Long-profile evolution of transport-limited gravel-bed
1100 rivers, *Earth Surf. Dynam.*, 7, 17–43, <https://doi.org/10.5194/esurf-7-17-2019>, 2019.
- 1101
1102 Wittmann, H., and von Blanckenburg, F.: Cosmogenic nuclide budgeting offloodplain
1103 sediment transfer. *Geomorphology*, 109, 246–256, 2009.
- 1104
1105 Wittmann, H., von Blanckenburg, F., Maurice, L., Guyot, J., Filizola, N., and Kubik, P.W.:
1106 Sediment production and delivery in the Amazon River basin quantified by in situ-produced
1107 cosmogenic nuclides and recent river loads. *GSA Bulletin*, 123 (5-6), 934–950, doi:
1108 <https://doi.org/10.1130/B30317.1>, 2011.
- 1109